NASA TECHNICAL NOTE

NASA TN D-2079

N64-10467

NASA TN D-2079

EXPERIMENTAL INVESTIGATION OF THE BEHAVIOR OF A CONFINED FLUID SUBJECTED TO NONUNIFORM SOURCE AND WALL HEATING

by Bernhard H. Anderson and Michael J. Kolar

Lewis Research Center
Cleveland, Ohio

NATIONAL AERONAUTICS AND SPACE ADMINISTRATION • WASHINGTON, D. C. • NOVEMBER 1963

TECHNICAL NOTE D-2079

EXPERIMENTAL INVESTIGATION OF THE BEHAVIOR OF A CONFINED FLUID SUBJECTED TO NONUNIFORM SOURCE AND WALL HEATING

By Bernhard H. Anderson and Michael J. Kolar

Lewis Research Center
Cleveland, Ohio

NATIONAL AERONAUTICS AND SPACE ADMINISTRATION

EXPERIMENTAL INVESTIGATION OF THE BEHAVIOR OF A CONFINED FLUID SUBJECTED TO NONUNIFORM SOURCE AND WALL HEATING

By Bernhard H. Anderson and Michael J. Kolar

SUMMARY

The motion of a fluid contained in a tank was studied under the following heating conditions: (1) nonuniform source heating in which most of the heat is generated near the tank bottom, (2) wall heating, and (3) nonuniform source heating in conjunction with wall heating. Data was obtained under nonflowing and flowing conditions.

Where nonuniform source heating was present, the results indicated that there was mixing such that a constant temperature in the axial direction was produced. Wall heating always produced a stable temperature gradient near the liquid surface, which tended to be carried with the fluid during discharge. The two modes of heating, acting in conjunction with each other, tended to form two regions where the characteristic effects of each were dominant.

For nonuniform source heating, the temperature-time histories measured at the tank exit during fluid discharge could be predicted adequately by using a complete mix analysis. The temperature profile in the stratified layer, which was covered by wall heating, tended to be carried with the fluid during discharge and appeared to exhibit the property of similarity.

INTRODUCTION

One of the major anticipated problems encountered in the operation of manned or unmanned nuclear space vehicles using liquid hydrogen is the heating of the propellant by nuclear and thermal radiation. The heat input to the propellant may require additional shielding or insulation of the tank to prevent excessive temperature rise or boiling; however, this results in an increase in the gross weight of the vehicle. Increasing the tank pressure to compensate for the increase in propellant temperature would also add to the gross weight of the vehicle in the form of heavier tank walls. The liquid hydrogen temperature profile, and thus the amount of shielding or insulation required, depends on the manner in which the heat input is eventually distributed within the propellant by convective motion of the fluid. Even if the shield or tank weights are not increased, a thorough understanding of propellant heating will be needed to guarantee safe noncavitating performance in the propellant pumping system.

The propellant receives nuclear radiation from gammas and neutrons that leak out of the reactor and by capture gammas that are born in the hydrogen when thermal neutrons are absorbed. Nuclear radiation has the effect of increasing the kinetic energy of a molecule. This increase in kinetic energy is felt locally in the form of heat. Thus, nuclear radiation is characterized as source heating, which is nonuniform because of the absorption properties of the medium. In a propellant tank, heat generation will be greatest near the tank bottom and will decrease exponentially with distance away from the bottom.

The vehicle will also receive thermal radiation from three sources: direct solar radiation, planetary radiation, and albedo or reflected radiation. This heats the tank wall, which in turn gives up heat to the liquid inside by a convection process.

Thus, the total tank heating is a combination of nonuniform source heating through the tank bottom and convective heating from the tank walls. No information is available on the distribution of energy within a tank under these conditions. Therefore, an experiment was carried out at the Lewis Research Center to determine qualitatively the effects of wall heating alone, nonuniform source heating alone, and a combination of the two. A simple apparatus was designed that permitted direct visual observation, schlieren photographs, and a limited number of temperature measurements. Particular emphasis was placed on studying the bulk mixing process by observation of the fluid through the schlieren system.

In addition, a comparison was made between the data obtained in the experiment and an existing theory for predicting the outlet temperature-time history of the fluid in the case of nonuniform source heating. A study was also made of the similarity of dimensionless temperature profile within the tank in the case of wall heating.

APPARATUS AND PROCEDURE

This experiment was designed primarily to permit a visual inspection of fluid behavior induced by wall and nonuniform source heating. The influence on the heat transport and the velocity field due to these modes of heating was viewed by means of a schlieren system.

Figure 1 is a schematic diagram of the experimental arrangement consisting of a two-dimensional glass tank, infrared heating lamps, and a support structure. The sides and bottom of the tank were fabricated of 1/8-inch-thick Pyrex plate glass, and the front and back plates of the tank (through which the fluid motion was viewed) consisted of 1/4-inch-thick Pyrex plate glass. The glass sections of the tank were held together with Epoxy. The glass view tank was 12 inches high, 8 inches wide, and 2 inches deep (inside dimensions); the bottom portion of the tank had 4.24-inch-long sides that were set at an angle of 45° with respect to the tank axis. An outlet port was located in the bottom glass plate to permit the fluid to discharge. Access ports were located in the top of the tank for the fluid fill line, the vent line, and the instrumentation. Three 1000-watt in-

frared lamps, located as shown in figure 1, provided a variable heat input to the fluid. Each lamp was provided with a parabolic reflector to ensure a monodirectional radiation source and to increase the heating efficiency of the lamps. The two vertical side walls of the tank were blackened down to the slant section to provide uniform-type wall heating. The bottom section was clear; thus the infrared radiation was allowed to penetrate the tank and be absorbed by the fluid.

The flow system was composed of a rotameter, a metering valve, and two reservoirs, one located 15 feet below the view tank while the other was about 3 feet above the view tank. The fluid was allowed to discharge out of the tank by the action of gravity; this was controlled by the metering valve and measured by a rotameter. The lower reservoir was used as a storage location before the fluid was pumped to an upper reservoir for future runs.

Infrared Absorption

The infrared region of the electromagnetic spectrum extends from wavelengths of about 0.75 to 1000 microns. Infrared rays are a form of electromagnetic radiation, which when absorbed by a liquid causes molecular agitation. This increase in kinetic energy of the molecule is felt locally in the form of heat (for further information, see ref. 1).

The absorption of infrared radiation in a fluid displays the characteristic exponential-type attenuation with distance into the fluid that is encountered with the absorption of nuclear radiation in hydrogen. The infrared attenuation profile within a fluid depends on the spectral energy distribution of the source and the spectral absorption characteristics of the liquid. The spectral energy distribution of the 1000-watt infrared lamps used in this experiment is presented in figure 2, which shows radiant power as a function of wavelength for full-power operation. The spectral absorption and, hence, the attenuation profile, can be controlled to some extent by mixing fluids with different absorption characteristics. For this experiment, a solution of 2 parts trichloroethane to 1 part ethyl alcohol by volume was used as the working fluid. The properties of the working fluid are presented in table I.

Because of the geometry of the tank bottom, the infrared attenuation varied in the radial direction. The exit port acted as a shield for infrared radiation, which caused the lines of constant intensity to fall off at the tank axis. This is illustrated in figure 3, which presents lines of constant infrared intensity, as measured with a radiometer.

The intensity measurements were obtained at six radial locations for a given liquid level. The liquid level was then changed, and the measurements were repeated. The intensity measurements presented in figure 3 were referenced to the intensity at the inside tank wall. The amount of heat absorbed in the glass was between 15 to 20 percent of the total incident flux. For a nuclear vehicle, it has been estimated that about 1 percent of the total heat generation will occur in the tank walls.

Heat Absorption Measurements

Nonuniform source heating. - The presence of radial heating gradients in the fluid, together with the severe anomaly that was shown to exist along the tank centerline, makes any comparison of measured attenuation difficult. Therefore, the infrared attenuation profile through the fluid will be characterized as the average heating rate in the cross section at any axial station measured from the tank bottom.

The average infrared heat generation as a function of distance from the tank bottom (fig. 4) was constructed from measurements (with a shielded thermocouple) of the average temperature rise per unit time for incremental changes in fluid volume in a nonflowing system. These average measurements could be obtained because of bulk mixing that occurred with nonuniform heating of the fluid. This will be discussed in the section Nonuniform source heating (see RESULTS AND DISCUSSION). Because a temperature gradient, which may have been caused by heat deposition in the glass, formed in a thin region of fluid near the tank bottom, the infrared heat generation could not be reliably determined in the first quarter inch of the fluid. Since the heat generation near the tank bottom could not be measured, the total amount of nonuniform heat imposed is not known. Wherever the magnitude of the source heating is referred to in this report, the term will be used to mean the rate of heat absorption at the liquid level 9.50 inches above the tank bottom.

Measurements to obtain the amount of radiation incident upon the tank were made only for one power setting. The other heating rates were assumed to be proportional to the lamp power.

Wall heating. - Integrating the energy balance equation, for which the only source of heat input is heat transfer from the wall, over the time to discharge t_{max} results in the following equation:

$$\int_0^{t_{max}} \int_0^{x_s} q_w x \, d\sigma \, dt = c_p \dot{w}_p \int_0^{t_{max}} \vartheta(0,t) dt = Q_l \tag{1}$$

where q_w is the wall heat flux, $d\sigma$ is the differential surface area, and t is time. Integrating the left-hand side of equation (1) for the tank geometry used in this experiment and assuming a constant wall heat flux q_w yield

$$q_w = \frac{c_p \dot{w}_p^2}{\alpha^2 \beta \rho (L - x_1)^2} \int_0^{t_{max}} \vartheta(0,t) dt \tag{2}$$

where α and β are the thickness and the width of the tank, respectively, and $(L - x_1)$ is the distance over which the heat was applied. Hence, the wall heating rate was computed from equation (2) by numerically integrating temperature-time data. This value of wall heating, however, accounts only for the heat that entered the fluid and does not include evaporation losses, which were large in some instances.

INSTRUMENTATION

Axial temperature measurements were made in the tank with 23 shielded thermocouples spaced one-half inch apart on a rake (see fig. 1). The shielding was necessary to prevent erroneous temperature measurements from the absorption of infrared radiation. A second rake, which is not shown, contained 20 unshielded thermocouples spaced one-tenth inch apart and was used to obtain the temperature profile in the vicinity of the liquid surface. Temperatures were recorded on three Leeds and Northrup recorders, each having 10 channels with a recording speed of 2 seconds per channel.

RESULTS AND DISCUSSION

Nonflowing System

The modes of applying heat to the fluid were divided into three categories, namely, nonuniform source heating, wall heating, and a combination of wall and nonuniform source heating. Comparison of the resulting axial temperature distributions at various times after start of heating are presented in figures 5 to 7. Schlieren photographs, which show the resulting flow patterns for the corresponding heating values, are presented in figures 8 to 10.

Nonuniform source heating. - The type in which most of the heating is produced near the bottom of an enclosed volume of fluid is analogous to heating of a horizontal layer from below in the sense that both produce an unstable stratification of warm fluid. This was originally studied by Rayleigh in 1916 (ref. 2). It is recognized that this unstable stratification must break down under certain conditions and lead to a cellular type of flow (refs. 3 to 6). These cells are typical for the laminar flow regime, while fully developed turbulent flow leads to irregular and unstable boundaries of upward and downward motion of fluid (ref. 7).

The primary effect of nonuniform source heating, namely, the instability of the flow, is demonstrated in figure 5. The results indicate that nonuniform source heating of the type produced by the absorption of infrared radiation caused the flow to become unstable and distributed the heat uniformly throughout the fluid in a turbulent manner except within a thin region near the tank bottom. This trend held true for three values of source heating: 55.5, 103.5, and 163.2 Btu per hour (figs. 5(a), (b), and (c), respectively). No restraints were placed on the free liquid surface; thus, the fluid was allowed to evaporate at atmospheric pressure. Schlieren photographs corresponding to the same heating values are presented in figure 8. Schlieren movies obtained at the same heating value indicated that the fluid was in a state of turbulent motion, with the general pattern of motion in the upward and downward directions. It should be noted, however, that, while the general motion was in the axial direction, there were velocity components in the radial direction. The general motion of the fluid was also characterized as varying with time in a random manner such that there were no prominent regions of either upflow or downflow. While it would be expected that random fluctuations in the temperature measurements would occur in a state of turbulent motion of the fluid, this was not indicated because the thermo-

couples and the recording equipment were not fast enough to record such variations.

Wall heating. - The conditions for this experiment were such that the wall temperature everywhere exceeded the ambient temperature of the fluid. This resulted in the fluid in the neighborhood of the wall having a lower density than the fluid far from the wall. Thus, because of the buoyancy force, there was established an upward flow of fluid in the neighborhood of the wall. Because of the presence of the free liquid surface, the flow of warmer fluid from the boundary layer accumulated above the main bulk of fluid and a temperature gradient in the axial direction was established. This is illustrated in figure 6, which shows the axial temperature distribution in the tank at various times after start of heating for wall heating rates of 3.49, 7.58, and 15.85 Btu per square inch per hour. The motion of the fluid was such that it always maintained a stable configuration, that is, a higher temperature or lower fluid density at the liquid surface. The development of the temperature gradients near the liquid surface was similar in nature for all three of the wall heating rates imposed on the fluid (fig. 6) except that the stratified or hot layer grew at a faster rate for higher heating values. A thin, highly turbulent region developed at the liquid surface (dotted lines in fig. 6), which can be seen in the corresponding schlieren photographs (fig. 9). This will be discussed in detail in the section Surface layer. The dot-dash lines in figure 6 indicate the extent of the region affected by the presence of wall heating, as determined on the basis of temperature measurements. As seen from figure 6, the depth of this region appears to approach some asymptotic value.

The presence of the temperature gradient caused a severe thickening of the boundary layer to occur in the stratified layer (figs. 9(b), (c), and (12)). The uniform rise in temperature that occurred below the stratified layer could be caused by a scattering component of infrared radiation and by heat introduced through the tank outlet from outside sources.

Nonuniform source heating and wall heating. - Figure 7 shows the results of a situation in which nonuniform source heating was acting on the fluid in conjunction with wall heating. These results indicate that two distinct flow regions developed (excluding the thin turbulent region near the liquid surface). In the upper portion of the tank, wall heating was the predominate source of heating, and the characteristic temperature gradient resulting from wall heating occurred. In the lower region of the tank, source heating prevailed resulting in a uniform temperature distribution. The rate of temperature rise in the lower region depends on the rate of growth of the stratified layer, which, in turn, depends on the magnitude of the wall heating in comparison with the magnitude of source heating. Nonuniform source heating produced turbulent mixing, with the general motion tending upward in the tank. The fluid continued to rise until it encountered a region of equal density, or temperature, at which time the body force became zero. Thus, the general motion of the fluid caused by nonuniform source heating was unable to penetrate through the stratified layer produced by wall heating. Increasing the wall heating, relative to the magnitude of source heating, tended to compress the region of uniform mixing (see fig. 10). This resulted in a smaller region over which the source heating could distribute itself and caused a higher temperature rise per unit time in the lower region.

From a comparison of figures 8 and 10, it can be seen that nonuniform source heating caused a severe boundary-layer thickening along the tank wall.

Surface layer. - In all cases where wall heating was present, a thin turbulent surface layer was formed at the liquid surface. This was caused by the interaction of the two boundary-layer flows meeting at the surface of the fluid. Axial temperature measurements were made in the vicinity of this surface layer and are presented in figure 11 for three values of wall heating: 3.49, 7.58, and 15.85 Btu per square inch per hour, respectively. The thickness of this surface layer at the center of the tank did not change appreciably either with time or over the range of wall heating values imposed on the fluid. It should be noted that the fluid was evaporating while these temperature measurements were made. It was postulated that the effect of evaporation was felt only within this surface layer. The change in the slope of the temperature profile was probably caused by both the effect of evaporation and the mixing. Schlieren photographs (fig. 12) showing the flow patterns near the liquid surface add to the description of this surface layer. These photographs show that the surface-layer thickness varied across the tank; this thickness was largest near the tank center and became thinner near the walls of the tank. A study of figure 12 indicates that the degree of mixing within this layer increased with increasing amounts of wall heating.

Formation of convection currents. - The discussion of the qualitative behavior of the fluid resulting from the three types of heating has been concerned primarily with the quasi-steady-state behavior of the convection currents. There is, however, a transient period in which the formation of the convection currents takes place. This occurs relatively rapidly, after which the quasi-steady-state behavior of the fluid exists.

Schlieren photographs showing the formation of the convection currents during the first 40 seconds are presented in figure 13. For nonuniform source heating (fig. 13(a)), there is, initially, a thermal boundary-layer buildup along the tank bottom including the sides set at 45° to the centerline. Between 10 and 15 seconds after the start of heating, the thermal boundary layer becomes unstable and a general turbulent flow of fluid up the side walls of the tank follows. After 25 seconds, the fluid swirls in toward the center of the tank, and a random mixing of the imposed heat follows. The transient formation of the convection currents caused by wall heating is shown in figure 13(b). Initially, a boundary layer was formed along the tank walls with the motion in the upward direction. The presence of the liquid surface turns the flow of fluid within the boundary layer toward the center of the tank. After 10 seconds, the two columns of fluid moving along the liquid surface meet in the center. In the remainder of the sequence of photographs, a violent downward motion of the fluid takes place. This turbulent core of fluid gradually thins out to the surface layer previously discussed. The formation of convection currents caused by both nonuniform source heating and wall heating is shown in figure 13(c). The breakup of the boundary layer along the tank bottom was essentially of the same character as it was with source heating alone. The flow of turbulent fluid up the tank walls forms after 10 seconds and tends to disrupt the wall boundary layer. Fifteen seconds after the start of heating, the violent downward motion of the fluid characteristic of wall heating occurs. The turbulent motion that follows quickly forms the characteristic steady-state configuration (see fig. 10), which was

previously discussed.

Flowing System

Figure 14 presents the axial temperature profiles that were measured in the fluid at various times after start of heating for a flowing system. The dot-dash line is an estimation of the surface temperature rise as the liquid level drops. The dashed lines indicate the temperature profiles where data were not obtained.

For wall heating alone (fig. 14(a)), the results indicate that, after an initial period, a steady-state gradient was established in the axial direction and tended to be carried by the fluid during discharge. A comparison of data obtained in a nonflowing system reveals that the qualitative temperature profile was not affected appreciably by discharging the fluid. The results are essentially the same when wall heating was acting in conjunction with source heating (fig. 14(b)). The region of temperature gradient tended to compress the lower region of uniform mixing during fluid discharge.

Temperature histories of the outflowing fluid, measured at the tank outlet, are presented in figures 15 to 18 for nonuniform source heating, wall heating, and wall heating acting in conjunction with source heating. An inspection of the results obtained with source heating (fig. 15) reveals no apparent change in the mixing process for heating values of 55.5, 103.5, and 163.2 Btu per hour (figs. 15(a), (b), and (c), respectively) and over a range of mass discharge rates from 51.3 to 160.5 pounds per hour. The convective motion of the fluid, which occurred in the nonflowing system, was, therefore, unaffected by discharging the fluid.

A comparison of outflow data obtained with wall heating alone (figs. 17(a) and 18(a)) with data obtained with wall and nonuniform source heating (figs. 17(b) and 18(b)) indicates that the temperature rise in the earlier portion of the curves was caused primarily by nonuniform source heating.

A summary of the outflow data obtained at the tank outlet appears in table II. The parameters Q_i and q_w are the magnitudes of the source and the wall heating, respectively, which were imposed on the fluid. The parameter Q_t, the total amount of heat that was absorbed in the fluid during discharge is given by equation (1). The last three columns of table II will be discussed in the section Nonuniform source heating.

Similarity Approach

The concept of similarity has its origin from geometry; that is, two bodies are considered similar if their linear dimensions are in constant ratio of each other. In addition to the aforementioned condition, however, physical similarity requires that all quantities involved in a pair of systems, such as temperature, velocity, force, and so forth, be in constant ratio of each other. The existence of similarity permits studies to be made of physical phenomena on small scale models and allows generalization of experimental results. The importance of sim-

ilarity in mathematical solutions lies in the fact that, for a given system, it suffices to find the solution only once in terms of the dimensionless variables.

Nonuniform source heating. - The principle concern in this report for the case of nonuniform source heating is the temperature-time history of the fluid as it exits from the tank. For this reason, similarity (for nonuniform source heating) will be defined as the property whereby two outlet temperature-time histories differ only by a scale factor. Therefore, in the case of such similarity, the temperature-time histories can be made congruent if they are plotted in coordinates that have been made dimensionless with reference to the scale factors.

Figure 19 presents temperature-time histories for nonuniform source heating that have been made dimensionless with respect to the scale factors based on the complete mix case (see appendix B). In order to make the temperature rise ϑ and the time t dimensionless, they were divided by the maximum temperature rise ϑ_{max} and the time required to discharge all the liquid in the tank t_{max}, respectively. The results indicate that similarity of flow exists based on the scale factors for complete mix, for values of source heating of 55.5, 103.5, and 163.2 Btu per hour and over a range of mass flow rates from 51.3 to 160.5 pounds per hour. In spite of the temperature gradient near the tank bottom, the property of similarity was not altered.

Comparison of these data with theoretical calculations based on a measured heat attenuation is presented in figure 20. Because of the inability to measure the attenuation in the region near the tank bottom, the temperature rise and the time were divided by the conditions at 0.968 of t_{max} to make them dimensionless. This is in keeping with the theory of complete mix (see appendix B). The results indicate that close agreement exists on a dimensionless basis between these data and the theoretical calculations. The absolute temperature rise ϑ_{ref} calculated from the theory of complete mix always tended to be lower than the measured values (table II). This is due, in part, to the fact that the temperature gradient near the tank bottom was not considered in the calculations.

Wall heating. - The presence of wall heating alters the bulk mixing process, in comparison with nonuniform source heating, in the sense that it produces an axial temperature gradient. Since a mathematical solution is exceedingly difficult, one approach to determine similarity behavior is experimentation.

Because wall heating produces an axial temperature gradient, it would be expected that similarity properties would depend on the behavior of the temperature gradient under varying conditions. It also would be expected that similarity behavior only extends over regions in which the same physical phenomenon takes place; hence, the surface layer, which has been previously discussed, will be excluded from consideration of the temperature gradient caused by wall heating. On this basis, it was postulated that the product of the temperature difference across the stratified layer times the volume of the stratified layer at time t is proportional to the total heat that went into the stratified layer up to time t. Consistent with this assumption

$$\frac{T(x,t) - T_j(t)}{T_s(t) - T_j(t)} = f\left[\frac{x - x_j(t)}{x_s(t) - x_j(t)}\right] \tag{3}$$

is independent of time and wall-heating rate q_w where $T_s(t)$ is the temperature just below the surface layer at location x_s, $T_j(t)$ is the temperature of the unaffected region at location $x_j(t)$, and $T(x)$ is the temperature at a location x. If $\eta(x,t) = [x - x_j(t)]/[x_s(t) - x_j(t)]$ and $\psi(x,t) = [T(x,t) - T_j(t)]/[T_s(t) - T_j(t)]$, equation (3) becomes

$$\psi = f(\eta) \tag{4}$$

Figure 21 presents the results obtained when the nonflowing data involving wall heating alone and wall heating in conjunction with source heating were made dimensionless on this basis. Data are presented for three values of wall heating in Btu per square inch per hour. Each value of wall heating includes temperature profiles obtained over a range of time from 120 to 240 seconds after start of heating. The results indicate that the dimensionless temperature ψ is independent of time and the wall-heating rate q_w. A comparison of data for wall heating and wall heating in conjunction with nonuniform source heating indicates that there was little tendency for nonuniform source heating to alter the temperature profile in the stratified layer.

The data presented in figure 21 also give the functional relation between η and ψ. The integral $\int_0^1 \psi \, d\eta$ represents the constant of proportionality between the total heat Q_t in the stratified layer and the quantity $\rho c_p(T_s - T_0)(x_s - x_0)A$ where A is the cross-sectional area of the tank.

CONCLUSIONS

The motion of a fluid contained in a tank was studied under (1) nonuniform source heating, (2) wall heating, and (3) nonuniform source heating in conjunction with wall heating. Data obtained under nonflowing and flowing conditions indicate the following conclusions:

1. Nonuniform source heating in which most of the heat is generated near the tank bottom results in a complete mixing of the imposed heat and a uniform temperature profile in the axial direction.

2. Wall heating results in a flow of warm fluid up the tank walls that produces a stable temperature gradient near the liquid surface.

3. Nonuniform source heating acting in conjunction with wall heating for the conditions investigated results in an interaction of the two modes of heating in which the general motion caused by source heating is unable to penetrate through the stratified layer resulting from wall heating.

4. For the conditions investigated, the measured temperature-time histories obtained at the tank exit for nonuniform source heating indicate good agreement with the predicted histories from complete mix theory.

5. For those conditions where wall heating is present, the temperature gra-

dient near the liquid surface tends to be carried with the fluid.

6. The temperature profiles in the stratified layer appeared to exhibit the property of similarity over the time of measurement, which was not altered appreciably by the presence of nonuniform source heating.

Lewis Research Center
National Aeronautics and Space Administration
Cleveland, Ohio, August 16, 1963

APPENDIX A

SYMBOLS

A	cross-sectional area of tank, sq ft
c_p	specific heat, Btu/(lb)(^oF)
L	initial level of liquid surface, ft
Q_i	source heating rate, Btu/hr
Q_t	total heat absorbed by fluid, Btu
q_i	local source heating rate, Btu/(cu ft)(hr)
q_w	wall heat flux, Btu/(sq in.)(hr)
T	temperature, ^oF
t	time, sec
t_{max}	time to outflow, sec
t_{ref}	0.968 t_{max}, sec
V	initial volume of fluid, cu in.
$\dot{w}_p$	mass flow rate, lb/hr
x	axial distance measured from tank bottom, in.
x_s	location of liquid level measured from tank bottom, in.
x_1	axial distance at which wall heating was started, in.
α	thickness of tank
β	width of tank
η	dimensionless distance, $[x - x_0(t)]/[x_s(t) - x_0(t)]$
θ	dimensionless temperature rise defined by eq. (B16)
$\overline{\theta}$	dimensionless temperature rise defined by eq. (B18)
ϑ	temperature rise, ^oF
ϑ_{max}	temperature rise at t_{max}, ^oF
ϑ_{ref}	temperature rise at t_{ref}, ^oF

ρ density, lb/cu ft

σ surface area of tank, ft

τ dimensionless time defined by eq. (B17)

$\overline{\tau}$ dimensionless time defined by eq. (B19)

ψ dimensionless temperature difference, $[T(x,t) - T_0(t)]/[T_s(t) - T_0(t)]$

Subscripts:

i internal conditions

j conditions in the unaffected region

s surface conditions

w wall conditions

0 initial conditions

Superscript:

* dimensionless independent quantities

APPENDIX B

DERIVATION OF EQUATION FOR COMPLETE MIXING

Assume a nonuniform heat source distribution throughout the fluid that varies only in the axial direction with no other sources of heat loss or gain. It is also assumed that the resulting temperature gradient in the radial direction is zero. In addition, it is further assumed that the physical properties of the fluid do not vary significantly over the temperature range under consideration. The energy balance equation for this system expresses the fact that the rate of increase of enthalpy of the fluid is equal to the rate at which heat is generated within the fluid minus the rate at which enthalpy is transported out of the system. In equation form, this is expressed as

$$\rho c_p \frac{d}{dt} \int_0^{x_s(t)} \vartheta(x,t)A(x)dx = \int_0^{x_s(t)} q_i(x)A(x)dx - c_p\dot{w}_p\vartheta(0,t) \qquad (B1)$$

Differentiating the left-hand side of equation (B1) results in

$$\rho c_p \int_0^{x_s(t)} \frac{d\vartheta}{dt} A(x)dx + \rho c_p\vartheta(x_s,t)A(x_s) \frac{dx_s}{dt}$$

$$+ c_p\dot{w}_p\vartheta(0,t) = \int_0^{x_s(t)} q_i(x)A(x)dx \qquad (B2)$$

For complete mixing, the temperature distribution is assumed uniform throughout the fluid; hence, the temperature difference ϑ depends only on t, that is

$$\vartheta(x,t) = \vartheta(t) \qquad (B3)$$

Therefore, equation (B2) can be written as

$$\rho c_p \frac{d\vartheta}{dt} \int_0^{x_s(t)} A(x)dx + \rho c_p\vartheta(t)A(x_s) \frac{dx_s}{dt}$$

$$+ c_p\dot{w}_p\vartheta(t) = \int_0^{x_s(t)} q_i(x)A(x)dx \qquad (B4)$$

If the functional relation between the liquid level x_s and the time t is introduced in the following form:

$$\frac{dx_s}{dt} = - \frac{\dot{w}_p}{\rho A(x_s)} \qquad (B5)$$

equation (B4) becomes

$$\frac{d\vartheta}{dx_s} = - \frac{1}{c_p \dot{w}_p} A(x_s) \frac{\int_0^{x_s} q_i(x)A(x)dx}{\int_0^{x_s} A(x)dx} \tag{B6}$$

If the average $\overline{q}_i(x_s)$ is defined as

$$\overline{q}_i(x_s) = \frac{\int_0^{x_s} q_i(x)A(x)dx}{\int_0^{x_s} A(x)dx} \tag{B7}$$

equation (B6) becomes

$$\frac{d\vartheta}{dx_s} = - \frac{1}{c_p \dot{w}_p} A(x_s)\overline{q}_i(x_s) \tag{B8}$$

Integrating equation (B8) results in

$$\vartheta(x_s) = \frac{1}{c_p \dot{w}_p} \int_{x_s}^{L} \overline{q}_i(x_s)A(x_s)dx_s \tag{B9}$$

Equation (B5) can be integrated to obtain the following functional relation between x_s and t:

$$t = \frac{\rho}{\dot{w}_p} \int_{x_s}^{L} A(x)dx \tag{B10}$$

By dividing all linear dimensions by L, all areas by a reference area A_{ref}, and q_i by a reference local source heating rate $q_{i,ref}$, that is,

$$\left.\begin{aligned} x^* &= x/L \\ A^* &= A/A_{ref} \\ q_i^* &= q_i/q_{i,ref} \end{aligned}\right\} \tag{B11}$$

equations (B9) and (B10) become

$$\vartheta(x_s^*) = \frac{(q_i AL)_{ref}}{c_p \dot{w}_p} \int_{x_s^*}^{1.0} \overline{q}^* A^* \, dx_s^* \tag{B12}$$

$$t(x_s^*) = \frac{\rho(AL)_{ref}}{\dot{w}_p} \int_{x_s^*}^{1.0} A^* \, dx_s^* \tag{B13}$$

By introducing the reference temperature and the time defined by

$$\vartheta_{ref} = \frac{(q_i AL)_{ref}}{c_p \dot{w}_p} \int_{0}^{1.0} \overline{q}^* A^* \, dx_s^* = \vartheta_{max} \tag{B14}$$

$$t_{ref} = \frac{\rho(AL)_{ref}}{\dot{w}_p} \int_{0}^{1.0} A^* \, dx_s^* = t_{max} \tag{B15}$$

equations (B12) and (B13) become

$$\frac{\vartheta}{\vartheta_{max}} = \frac{\int_{x_s^*}^{1.0} \overline{q}^* A^* \, dx_s^*}{\int_{0}^{1.0} \overline{q}^* A^* \, dx_s^*} = \theta \tag{B16}$$

$$\frac{t}{t_{max}} = \frac{\int_{x_s^*}^{1.0} A^* \, dx_s^*}{\int_{0}^{1.0} A^* \, dx_s^*} = \tau \tag{B17}$$

Equations (B14) and (B15) express the fact that there is a similarity of the temperature-time history at the tank outlet, provided that geometrical similarity is preserved and $q_i/q_{i,ref}$ as a function of x/L is duplicated. Equations (B12) and (B13) can also be made dimensionless by introducing some other temperature difference ϑ along with the temperature history. For convenience, therefore, the temperature rise will be made dimensionless by dividing it by the conditions at 0.968 t_{max}; hence,

$$\overline{\theta} = \frac{\vartheta}{\vartheta_{ref}} = \frac{\int_{x_s^*}^{1.0} \overline{q}^* A^* \, dx_s^*}{\int_{x_{ref}^*}^{1.0} \overline{q}^* A^* \, dx_s^*} \tag{B18}$$

$$\bar{\tau} = \frac{t}{t_{ref}} = \frac{\int_{x_s^*}^{1.0} A^* \, dx_s^*}{\int_{x_{ref}^*}^{1.0} A^* \, dx_s^*} \tag{B19}$$

where x_{ref}^* can be determined from the equation

$$0.968 \, t_{max} = \frac{\rho(AL)_{ref}}{\dot{w}_p} \int_{x_{ref}^*}^{1.0} A^* \, dx_s^* \tag{B20}$$

REFERENCES

1. Holter, M. R., et al.: Fundamentals of Infra-Red Technology. The Macmillan Co., 1962.

2. Rayleigh: On Convection Currents in a Horizontal Layer of Fluid, When the Higher Temperature is on the Under Side. Phil. Mag. and Jour. Sci., ser. 6, vol. 32, no. 192, Dec. 1916, pp. 529-547.

3. Chandra, Krishna: Instability of Fluids Heated from Below. Proc. Roy. Soc. (London), ser. A, vol. 164, no. A917, Jan. 1938, pp. 231-242.

4. Schmidt, R. J., and Saunders, O. A.: On the Motion of a Fluid Heated from Below. Proc. Roy. Soc. (London), ser. A, vol. 165, no. A921, Apr. 1938, pp. 216-228.

5. Sutton, O. G.: On the Stability of a Fluid Heated from Below. Proc. Roy. Soc. (London), ser. A, vol. 204, no. 1078, Dec. 1950, pp. 297-309.

6. Bosworth, R. C. L.: Heat Transfer Phenomena. John Wiley & Sons, Inc., 1952.

7. Prandtl, Ludwig: Essentials of Fluid Dynamics. Hafner Pub. Co., 1952.

TABLE I. - PROPERTIES OF TEST FLUID

Fluid	Density, ρ, lb/cu ft	Specific heat, c_p, Btu/(lb)(^oF)
Ethyl alcohol, C_2H_5OH	49.2	0.616
Trichloroethane, CH_3CCl_3	82.6	.266
Solution of 2 parts CH_3CCl_3 and 1 part C_2H_5OH	71.3	.383

TABLE II. - SUMMARY OF TEST RESULTS

Source heating rate, Q_i, Btu/hr	Wall heat flux, q_w, Btu/(sq in.)(hr)	Mass flow rate, $\dot{w}_p$, lb/hr	Time to outflow, t_{max}, sec	Temperature rise at t_{max}, ϑ_{max}, ^oF	Total heat absorbed by fluid, Q_t, Btu	$t_{ref} = 0.968\ t_{max}$, sec	Temperature rise at t_{ref}, ϑ_{ref}, ^oF (a)	Temperature rise at t_{ref}, ϑ_{ref}, ^oF (b)
163.2	0	51.3	388	17.0	9.78	376	13.5	11.5
		104.8	190	7.0	-----	184	5.6	4.8
		160.5	124	3.4	-----	120	3.0	2.6
103.5	0	52.1	382	12.0	6.30	370	8.8	7.5
		102.6	194	6.2	-----	188	4.2	3.6
		153.0	130	4.2	-----	126	3.1	2.6
55.5	0	52.4	380	6.1	3.40	368	4.7	4.0
		103.6	192	3.1	-----	186	2.4	2.0
		153.0	130	2.0	-----	126	1.6	1.4
0	15.85	52.4	380	40.4	17.30	---	----	----
		102.6	194	25.4	-----	---	----	----
		165.8	120	16.6	-----	---	----	----
	7.58	51.6	386	22.0	8.42	---	----	----
		99.6	200	15.5	-----	---	----	----
		160.5	124	9.5	-----	---	----	----
	3.49	52.1	382	12.7	3.82	---	----	----
		101.5	196	8.7	-----	---	----	----
		160.5	124	5.2	-----	---	----	----
163.2	15.85	51.3	388	50.2	28.35	---	----	----
		104.8	190	28.7	-----	---	----	----
		165.8	120	17.5	-----	---	----	----
	7.58	51.6	386	28.9	16.3	---	----	----
		101.5	196	18.4	-----	---	----	----
		155.5	128	13.8	-----	---	----	----
	3.49	51.6	386	20.0	13.22	---	----	----
		101.5	196	10.6	-----	---	----	----
		155.5	128	7.6	-----	---	----	----

[a]Measured.

[b]Theoretical.

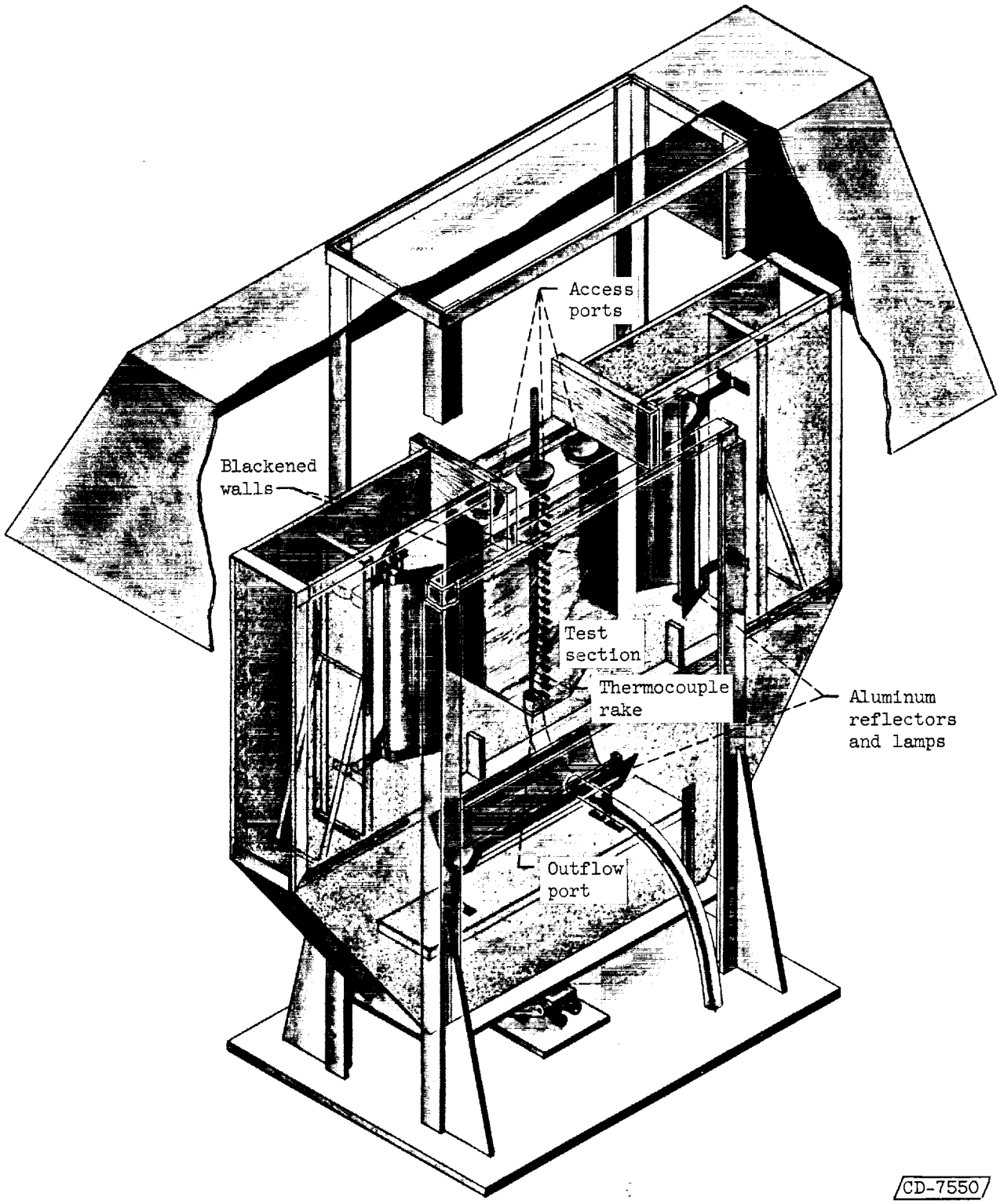

Figure 1. - Schematic diagram of test apparatus.

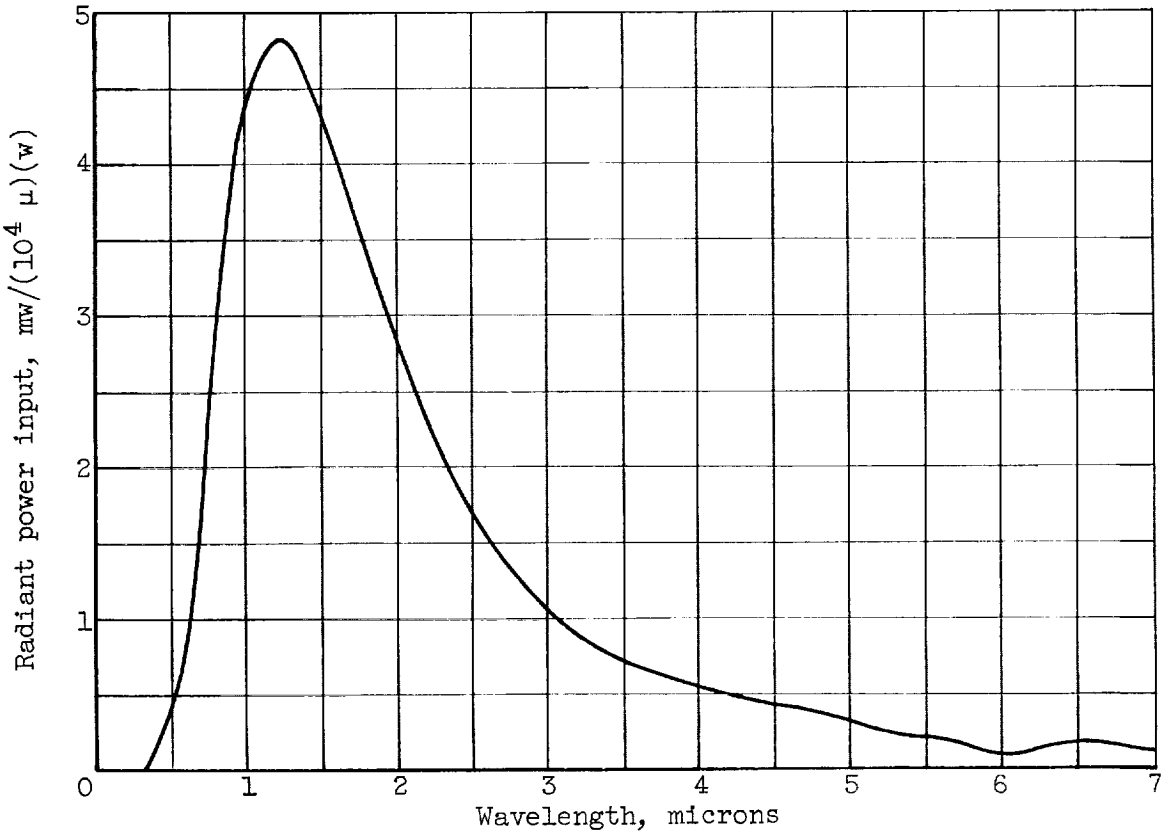

Figure 2. - Spectral energy distribution for 1000-watt infrared lamps.

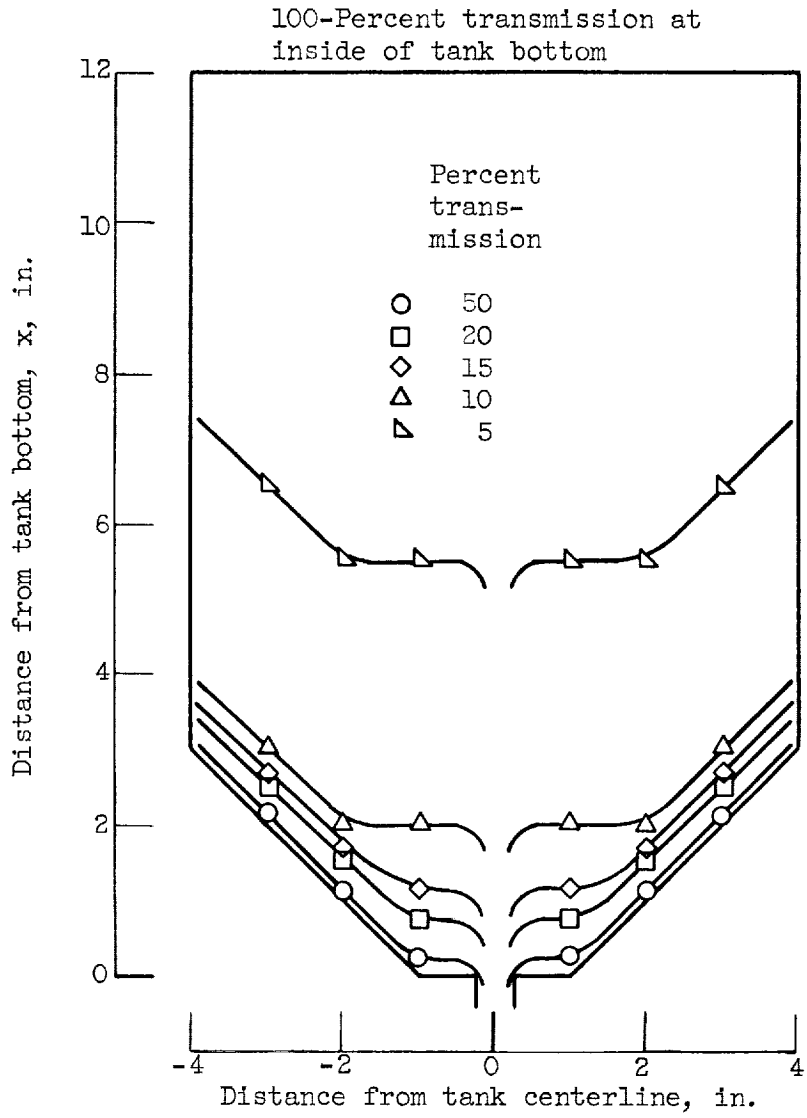

Figure 3. - Relative infrared radiation intensity measured in solution of 2 parts trichloroethane to 1 part ethyl alcohol.

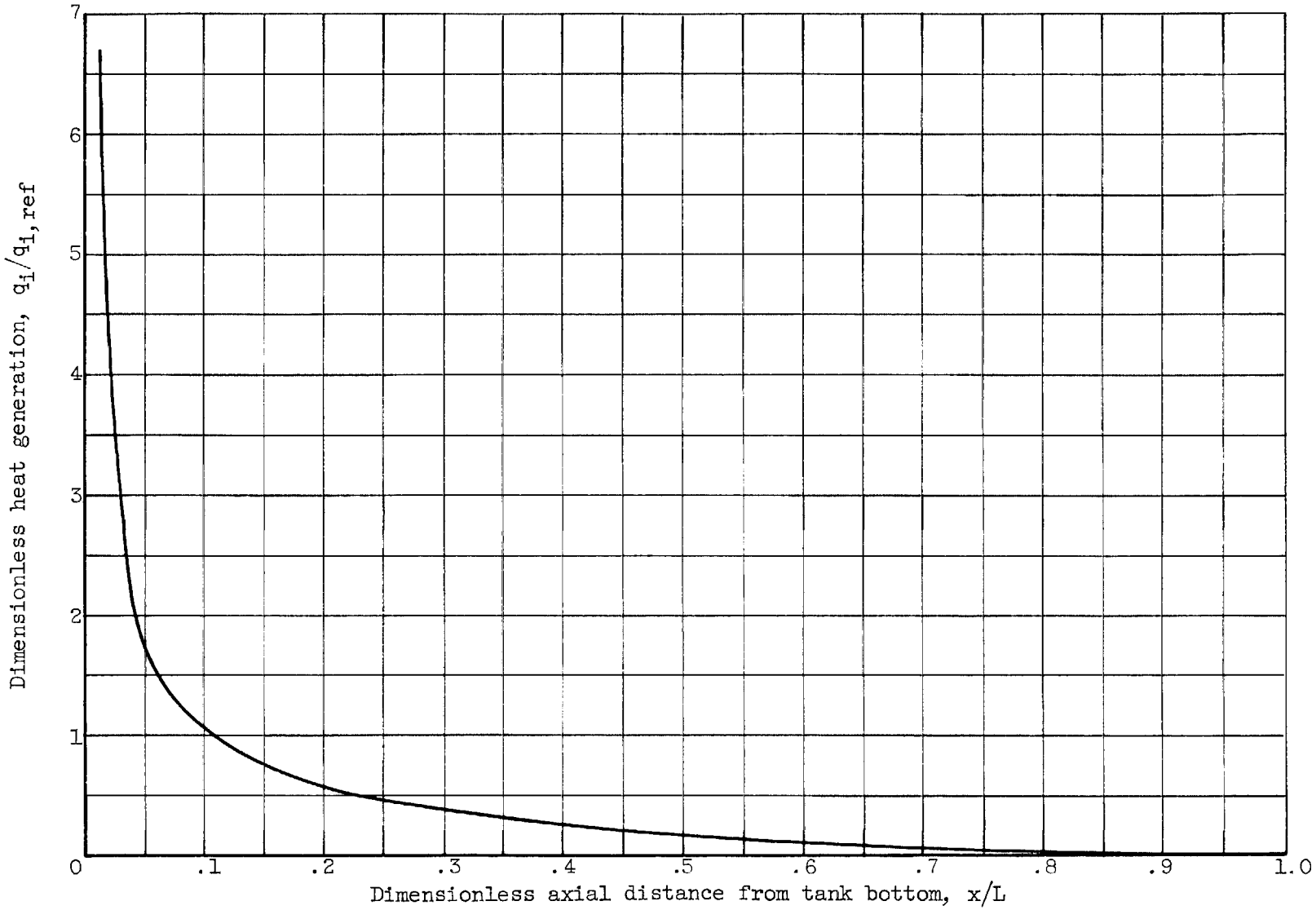

Figure 4. - Dimensionless plot of average infrared heat generation for solution of 2 parts trichloroethane to 1 part ethyl alcohol. Reference local source heating rate, 1.218 Btu per square inch per hour ($q_{i,ref} = Q_i/V$); initial level of liquid surface, 9.5 inches; source heating rate, 163.2 Btu per hour; initial volume of fluid, 134 cubic inches.

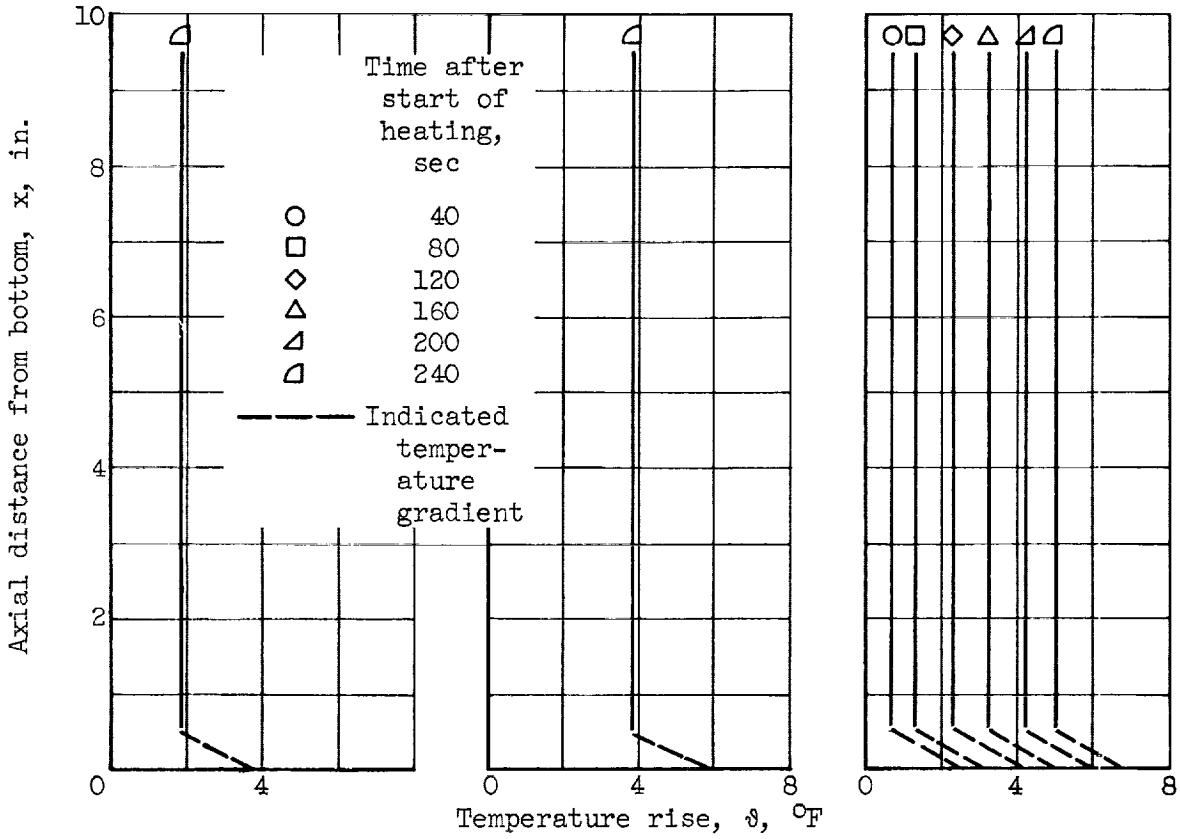

(a) Source heating rate, 55.5 Btu per hour.

(b) Source heating rate, 103.5 Btu per hour.

(c) Source heating rate, 163.2 Btu per hour.

Figure 5. - Axial temperature distribution with time for nonflowing system with nonuniform source heating.

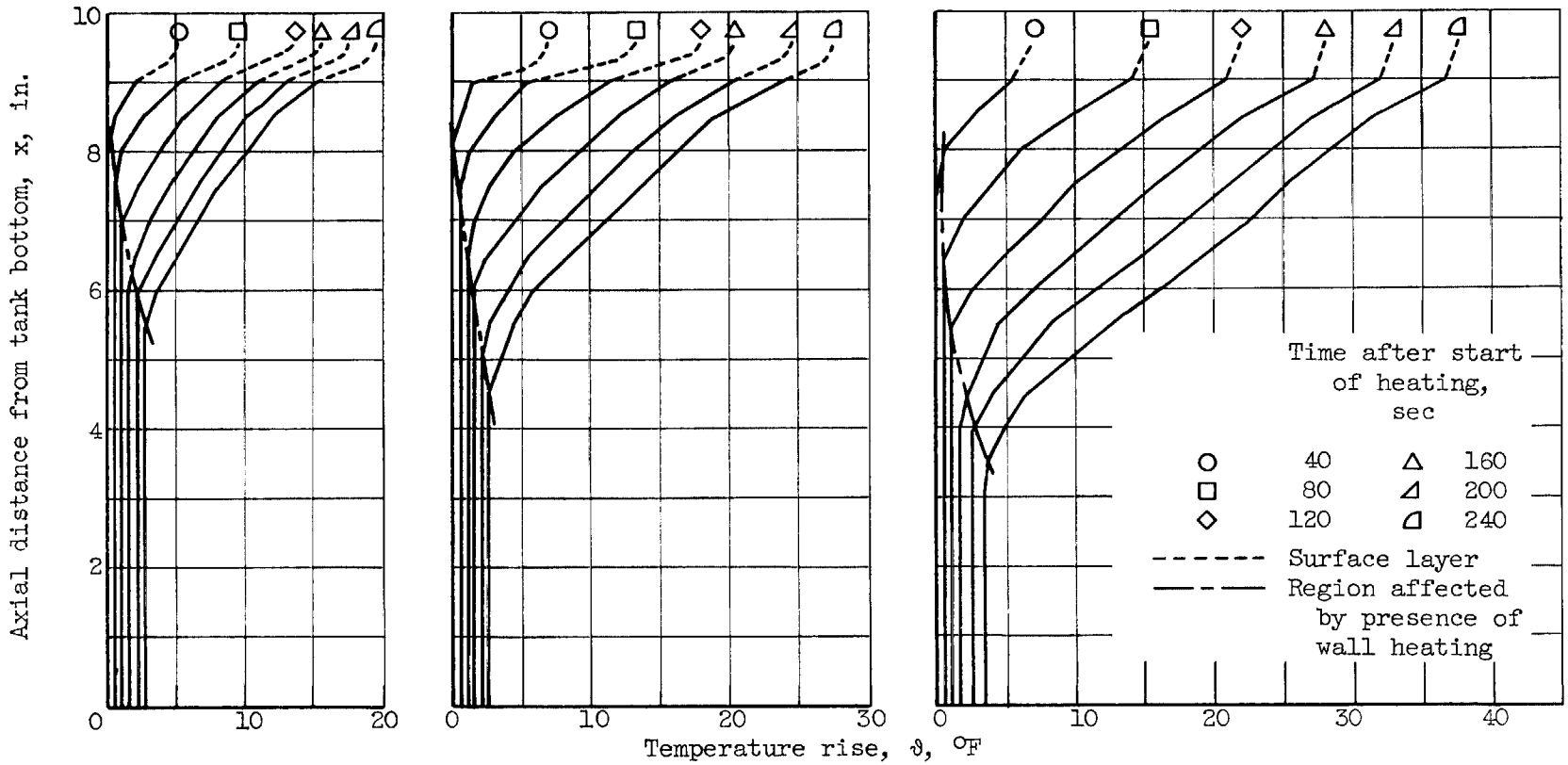

(a) Wall heat flux, 3.49 Btu per square inch per hour.

(b) Wall heat flux, 7.58 Btu per square inch per hour.

(c) Wall heat flux, 15.85 Btu per square inch per hour.

Figure 6. - Axial temperature distribution with time for nonflowing system with wall heating.

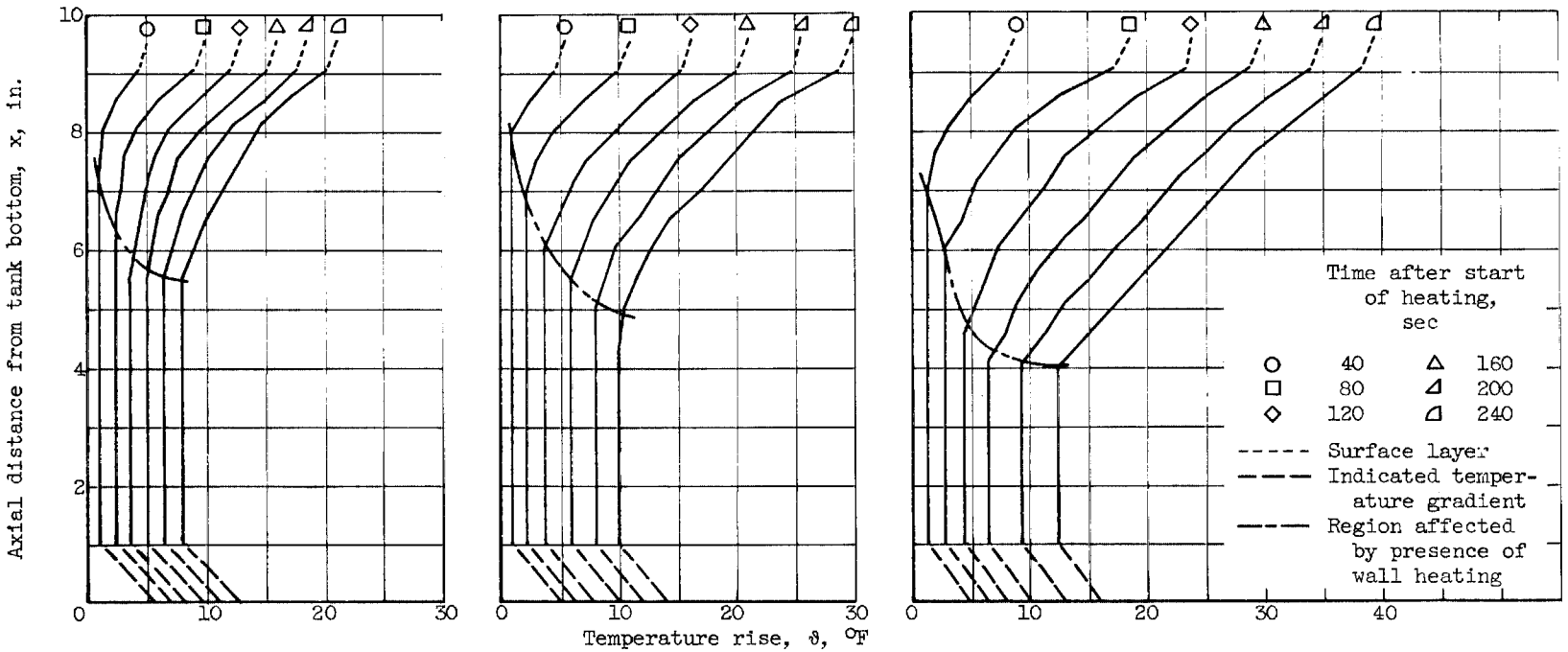

(a) Wall heat flux, 3.49 Btu per square inch per hour.

(b) Wall heat flux, 7.58 Btu per square inch per hour.

(c) Wall heat flux, 15.85 Btu per square inch per hour.

Figure 7. - Axial temperature distribution with time for nonflowing system, nonuniform source, and wall heating. Source heating rate, 163.2 Btu per hour.

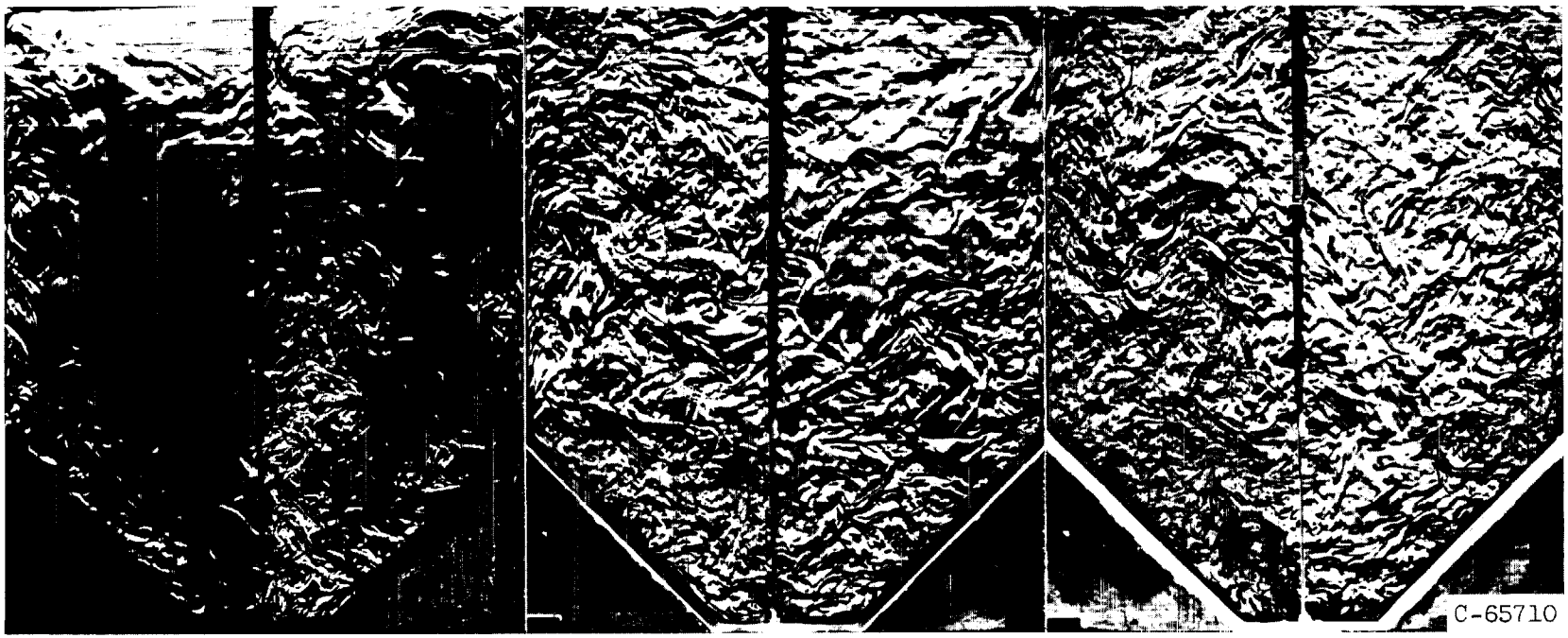

(a) Source heating rate, 55.5 Btu per hour.

(b) Source heating rate, 103.5 Btu per hour.

(c) Source heating rate, 163.2 Btu per hour.

Figure 8. - Schlieren photographs showing flow patterns resulting from nonuniform source heating.

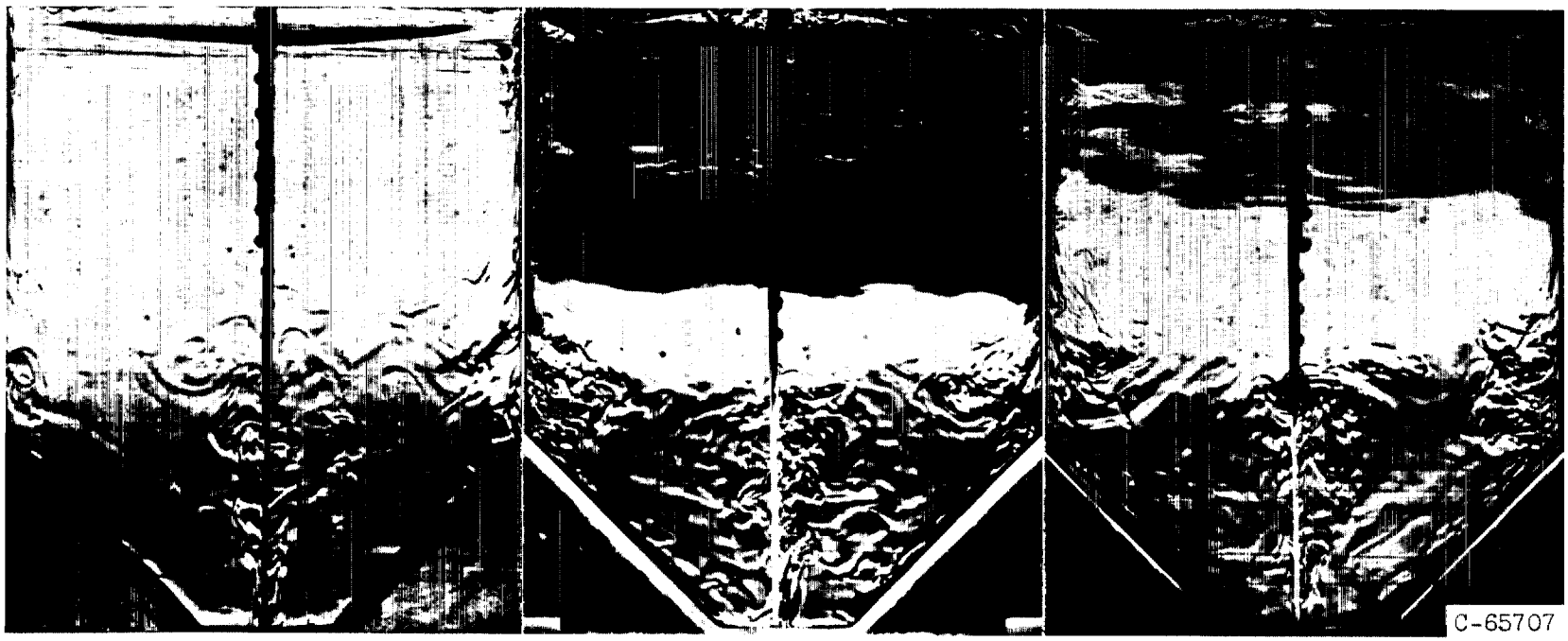

(a) Wall heat flux, 3.49 Btu per square inch per hour.

(b) Wall heat flux, 7.58 Btu per square inch per hour.

(c) Wall heat flux, 15.85 Btu per square inch per hour.

Figure 9. - Schlieren photographs showing flow patterns resulting from wall heating.

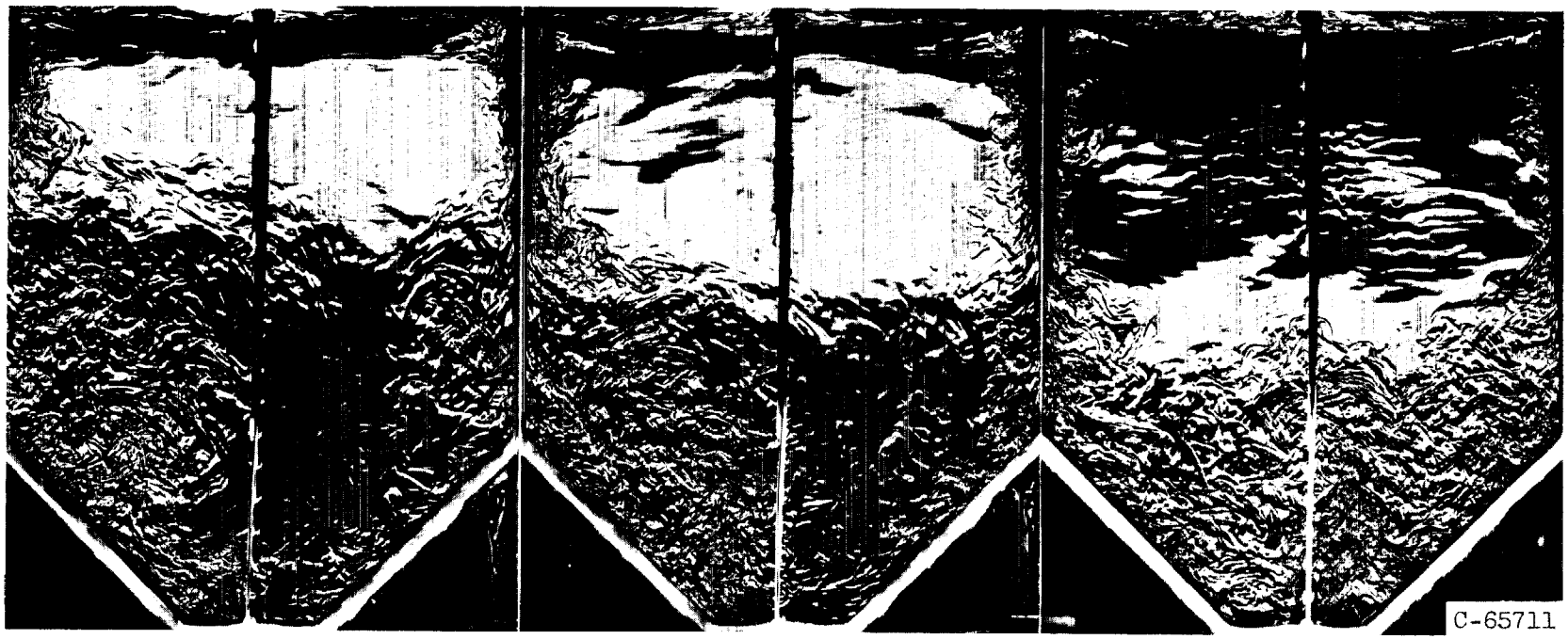

(a) Wall heat flux, 3.49 Btu per square inch per hour.

(b) Wall heat flux, 7.58 Btu per square inch per hour.

(c) Wall heat flux, 15.85 Btu per square inch per hour.

Figure 10. - Schlieren photographs showing flow patterns resulting from nonuniform source and wall heating. Source heating rate, 163.2 Btu per hour.

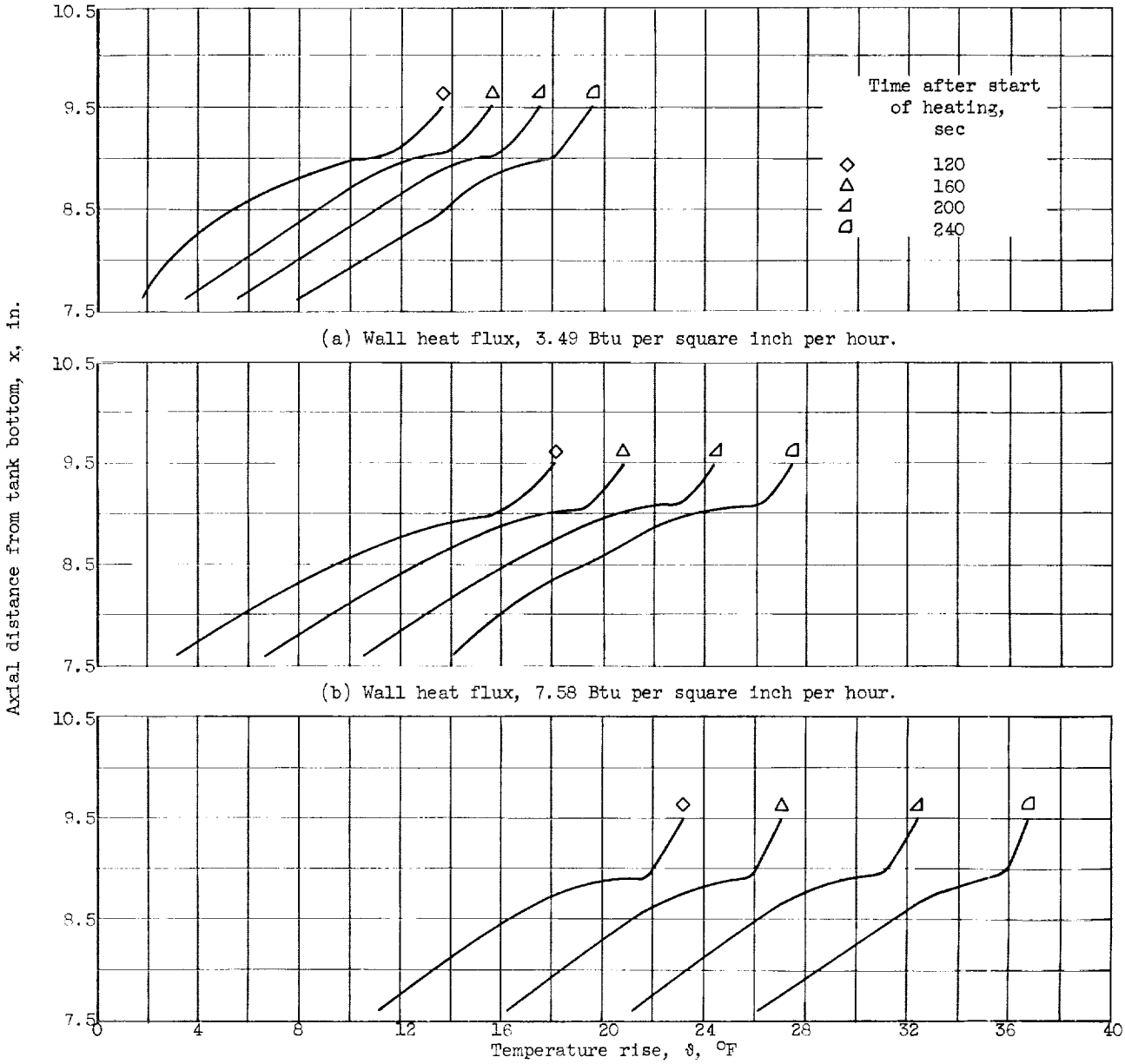

(a) Wall heat flux, 3.49 Btu per square inch per hour.

(b) Wall heat flux, 7.58 Btu per square inch per hour.

(c) Wall heat flux, 15.85 Btu per square inch per hour.

Figure 11. - Axial temperature distribution with time near liquid surface for nonflowing system with wall heating.

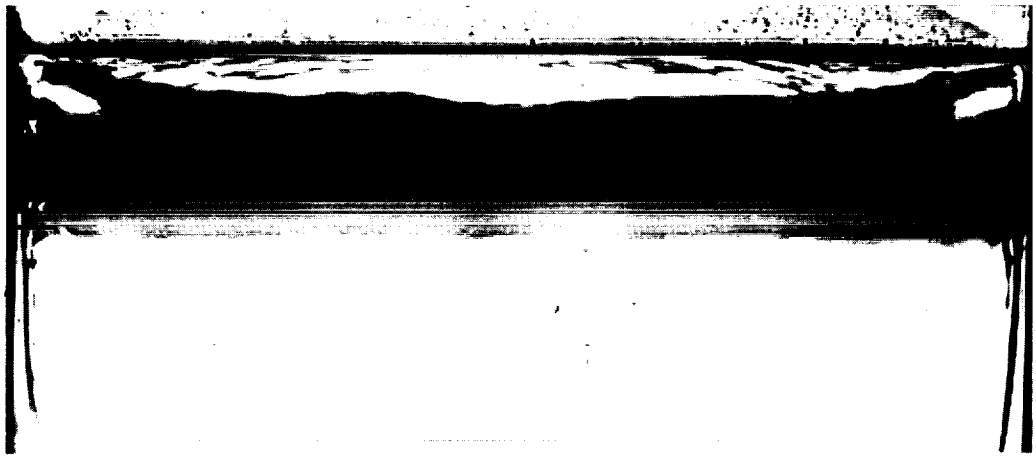

(a) Wall heat flux, 3.49 Btu per square inch per hour.

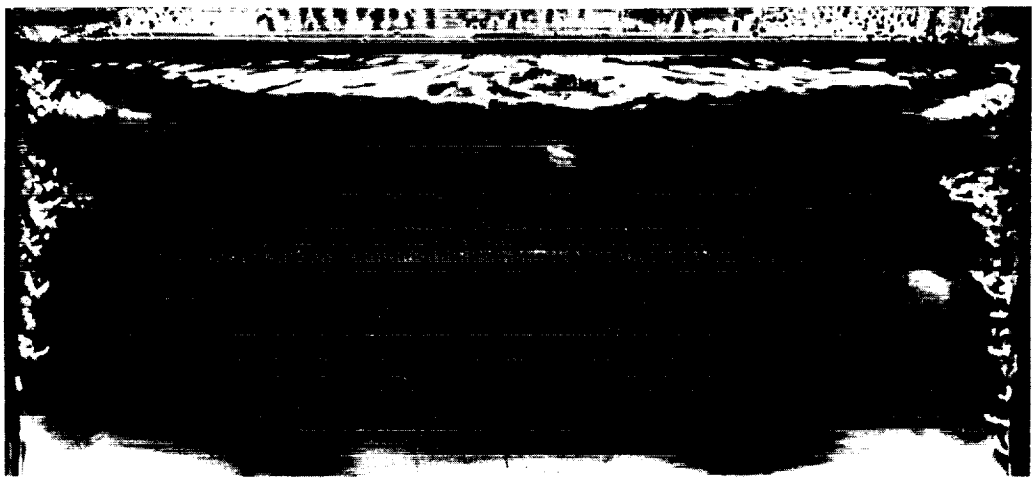

(b) Wall heat flux, 7.85 Btu per square inch per hour.

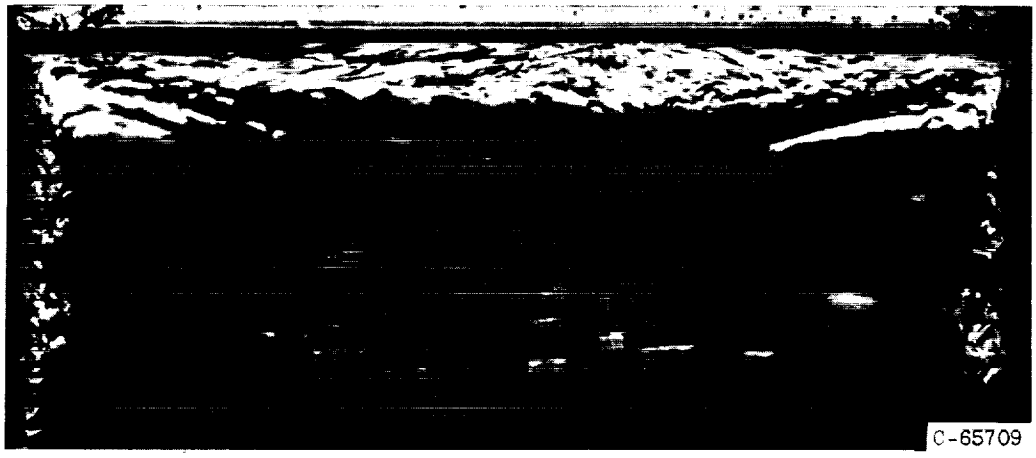

(c) Wall heat flux, 15.85 Btu per square inch per hour.

Figure 12. - Schlieren photographs showing flow patterns near liquid surface resulting from wall heating.

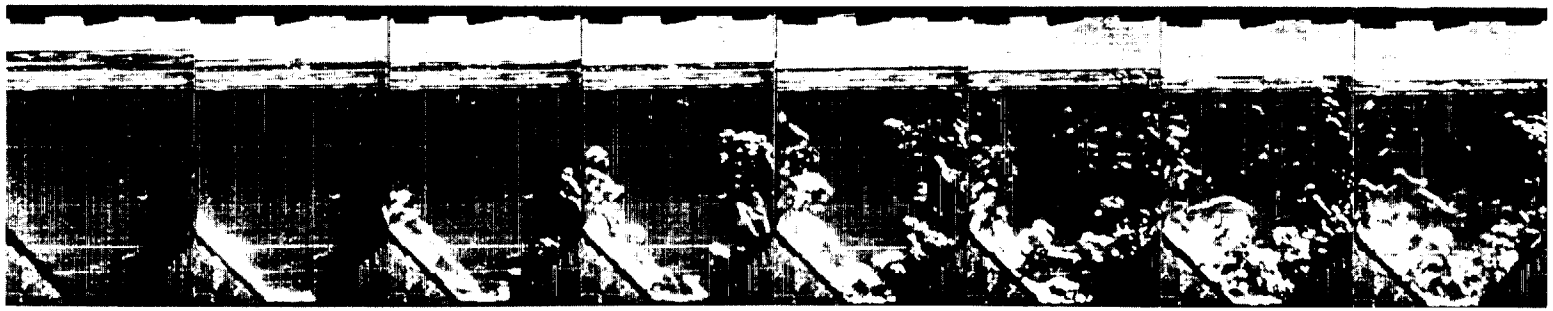

Time after start of heating, sec: 0 10 15 20 25 30 35 40

(a) Nonuniform source heating rate, 163.2 Btu per hour.

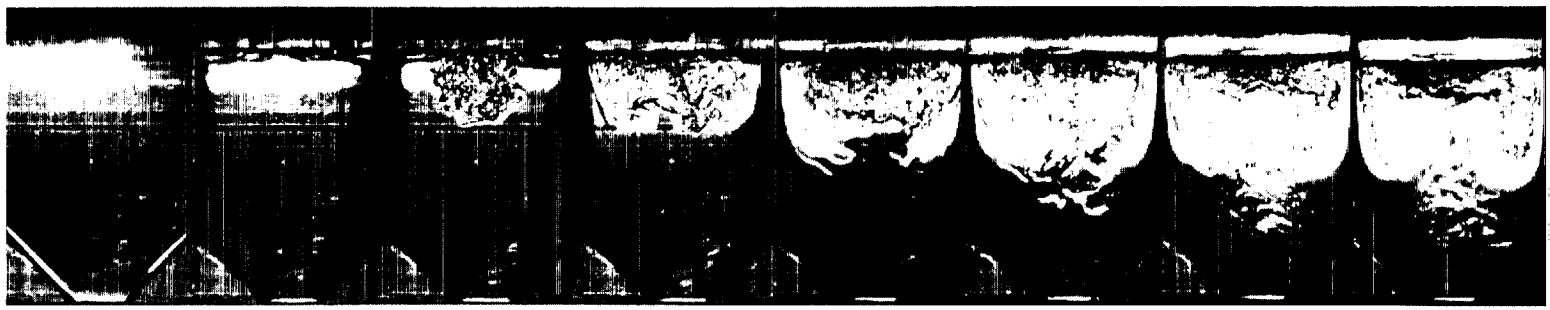

0 10 15 20 25 30 35 40

(b) Wall heat flux, 15.85 Btu per square inch per hour.

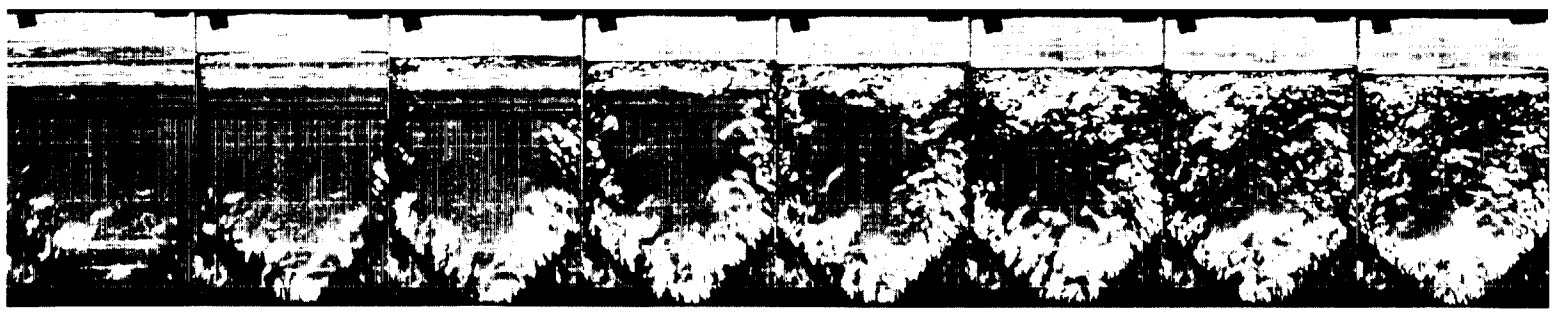

0 10 15 20 25 30 35 40

C-65708

(c) Nonuniform source heating rate, 163.2 Btu per hour; wall heat flux, 15.85 Btu per square inch per hour.

Figure 13. - Schlieren photographs showing formation of convection currents during outflow. Mass flow rate, 52.3 pounds per hour.

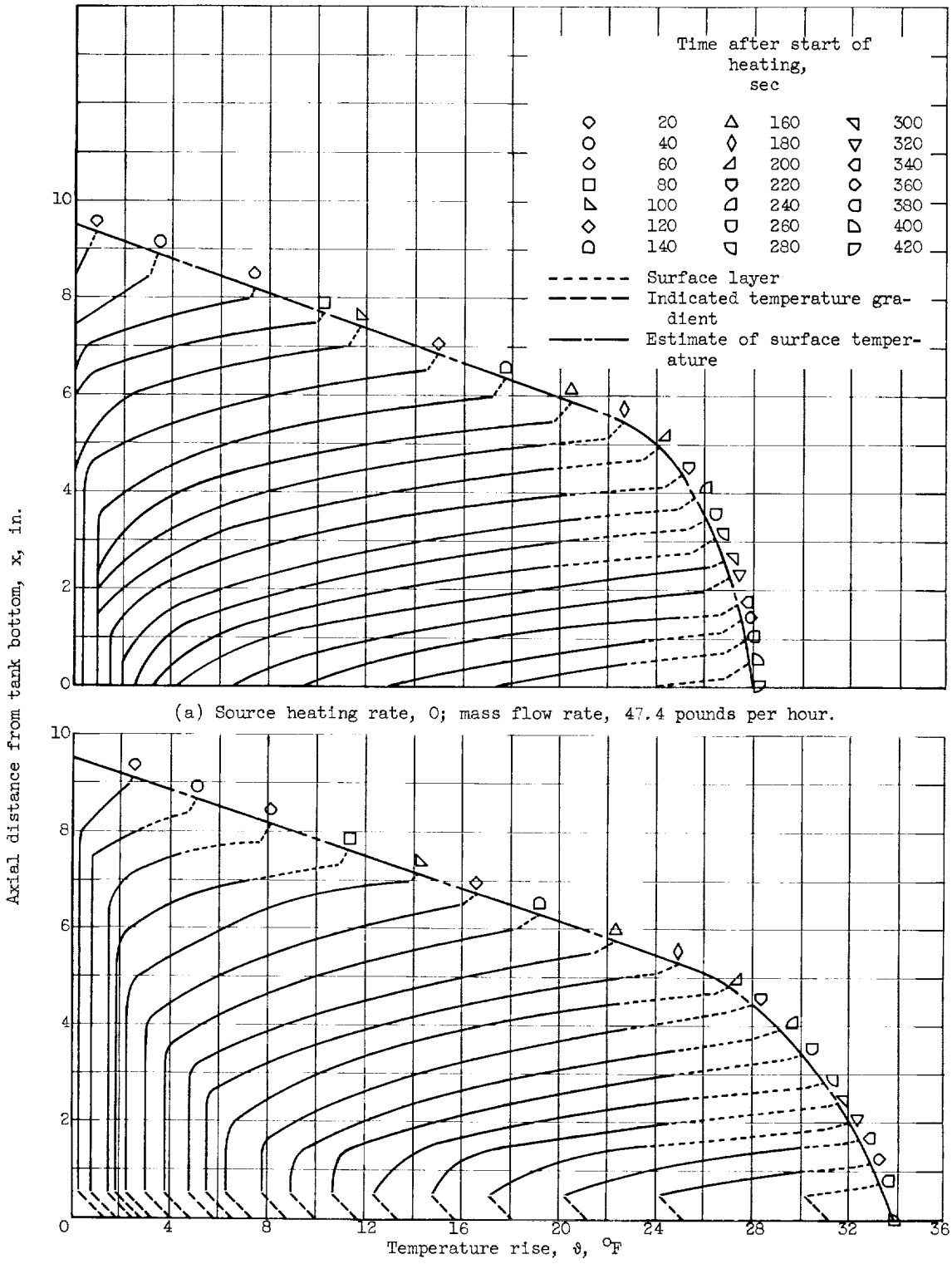

(a) Source heating rate, 0; mass flow rate, 47.4 pounds per hour.

(b) Source heating rate, 163.2 Btu per hour; mass flow rate, 49.8 pounds per hour.

Figure 14. - Axial temperature distribution with time for flowing system. Wall heat flux, 7.58 Btu per square inch per hour.

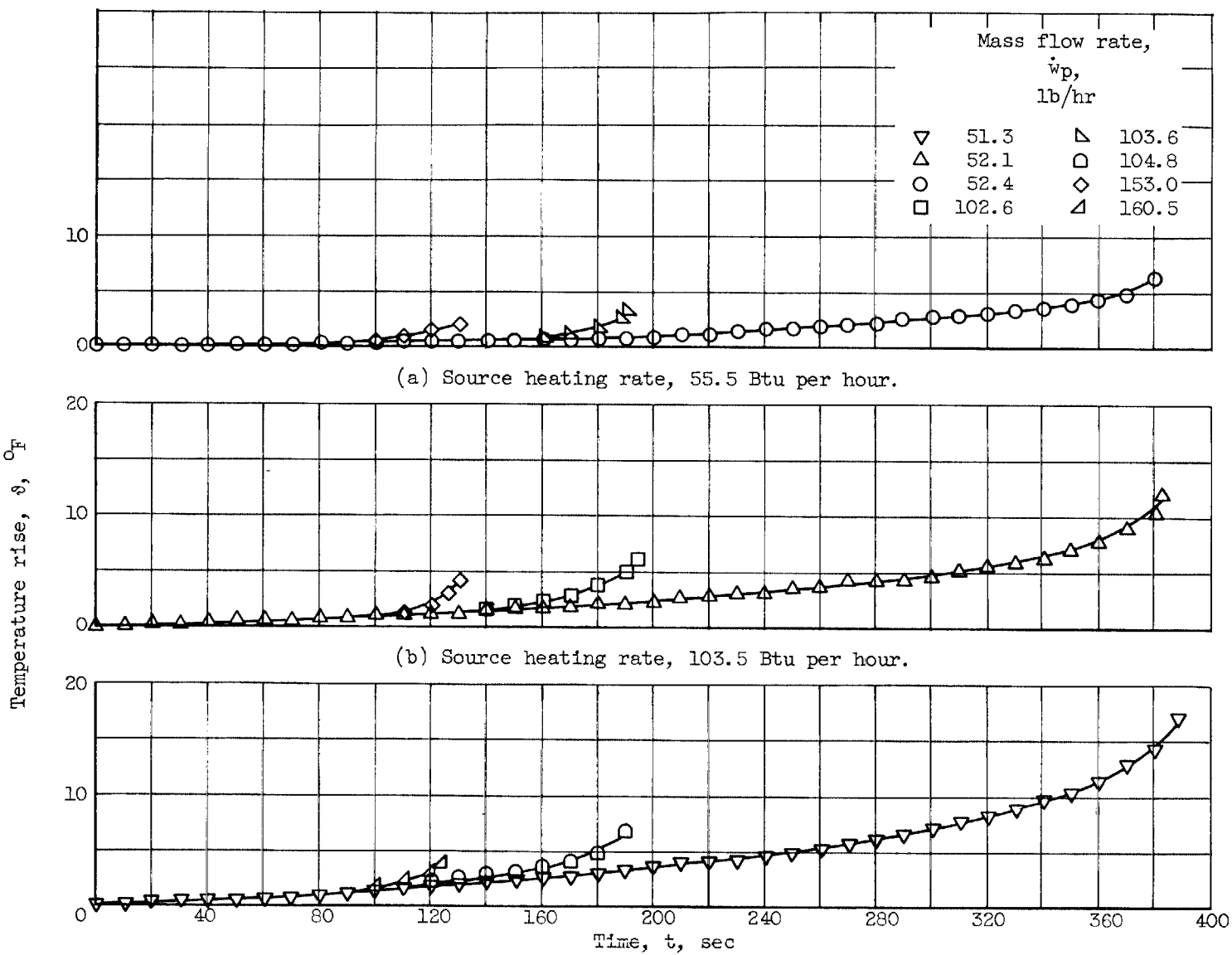

(a) Source heating rate, 55.5 Btu per hour.

(b) Source heating rate, 103.5 Btu per hour.

(c) Source heating rate, 163.2 Btu per hour.

Figure 15. - Temperature-time histories of outflowing fluid measured at tank exit for nonuniform source heating. Wall heat flux, 0.

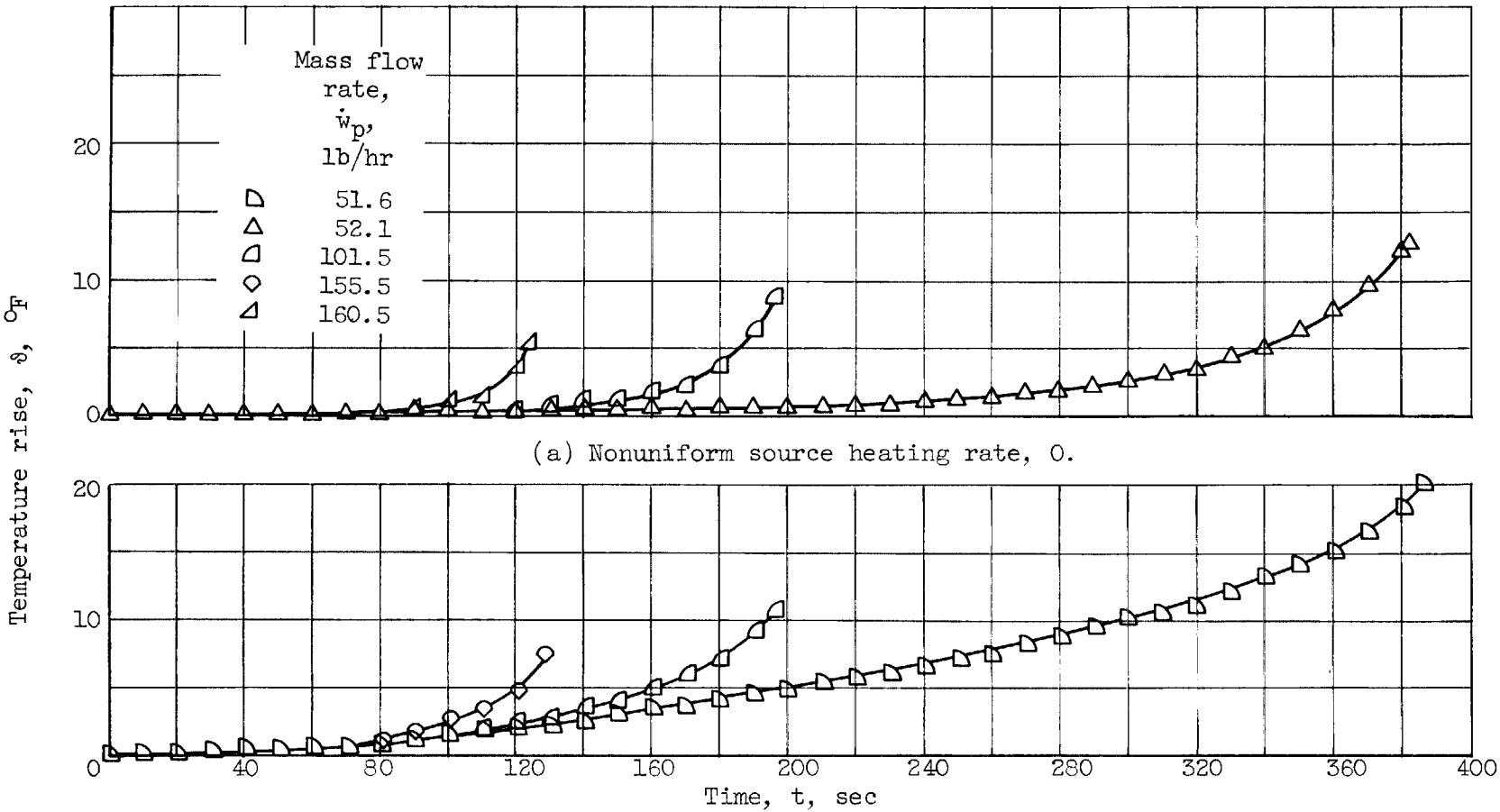

(a) Nonuniform source heating rate, 0.

(b) Nonuniform source heating rate, 163.2 Btu per hour.

Figure 16. - Temperature-time histories of outflowing fluid measured at tank exit. Wall heat flux, 3.49 Btu per square inch per hour.

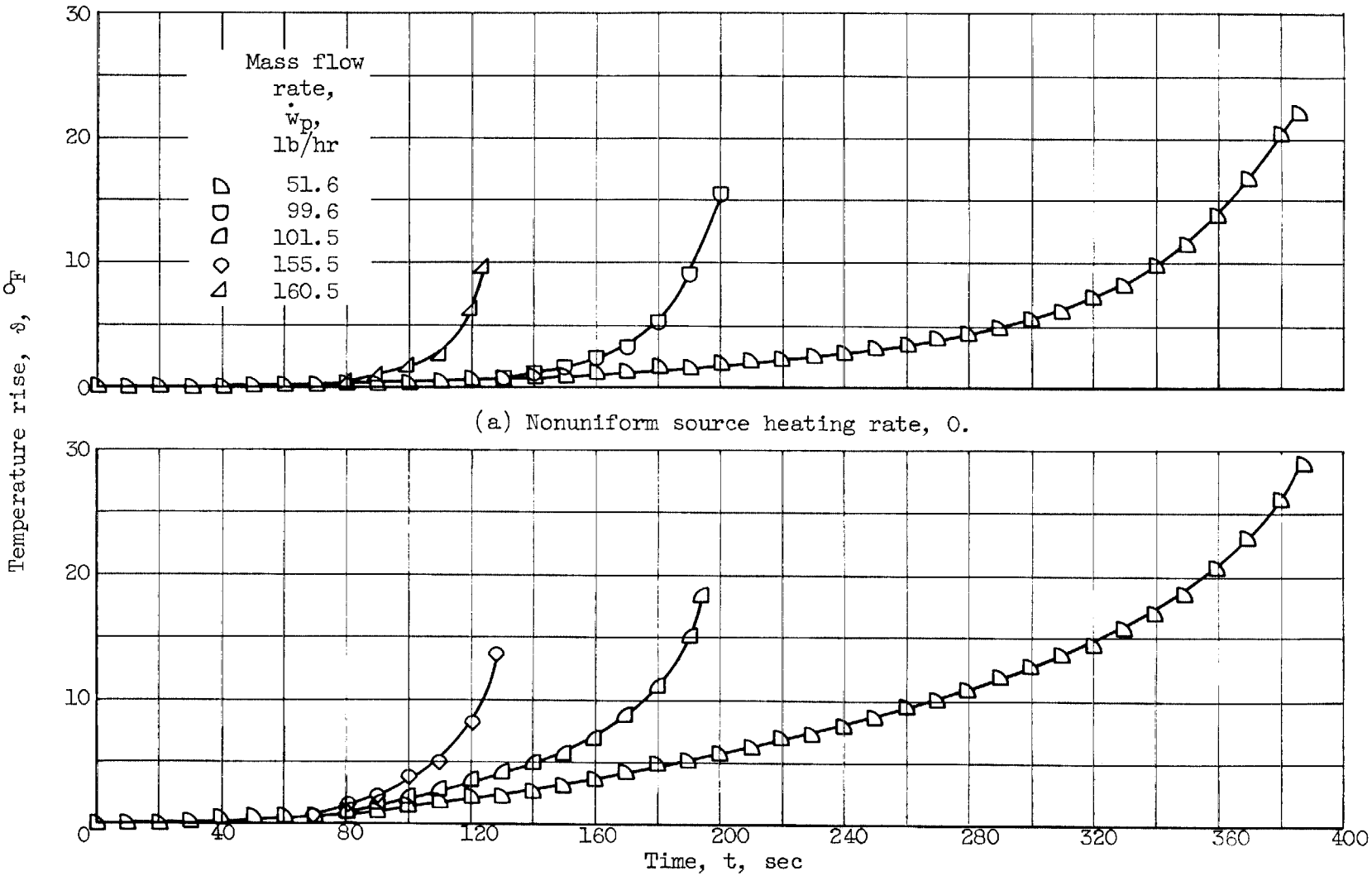

(a) Nonuniform source heating rate, 0.

(b) Nonuniform source heating rate, 163.2 Btu per hour.

Figure 17. - Temperature-time histories of outflowing fluid measured at tank exit. Wall heat flux, 7.58 Btu per square inch per hour.

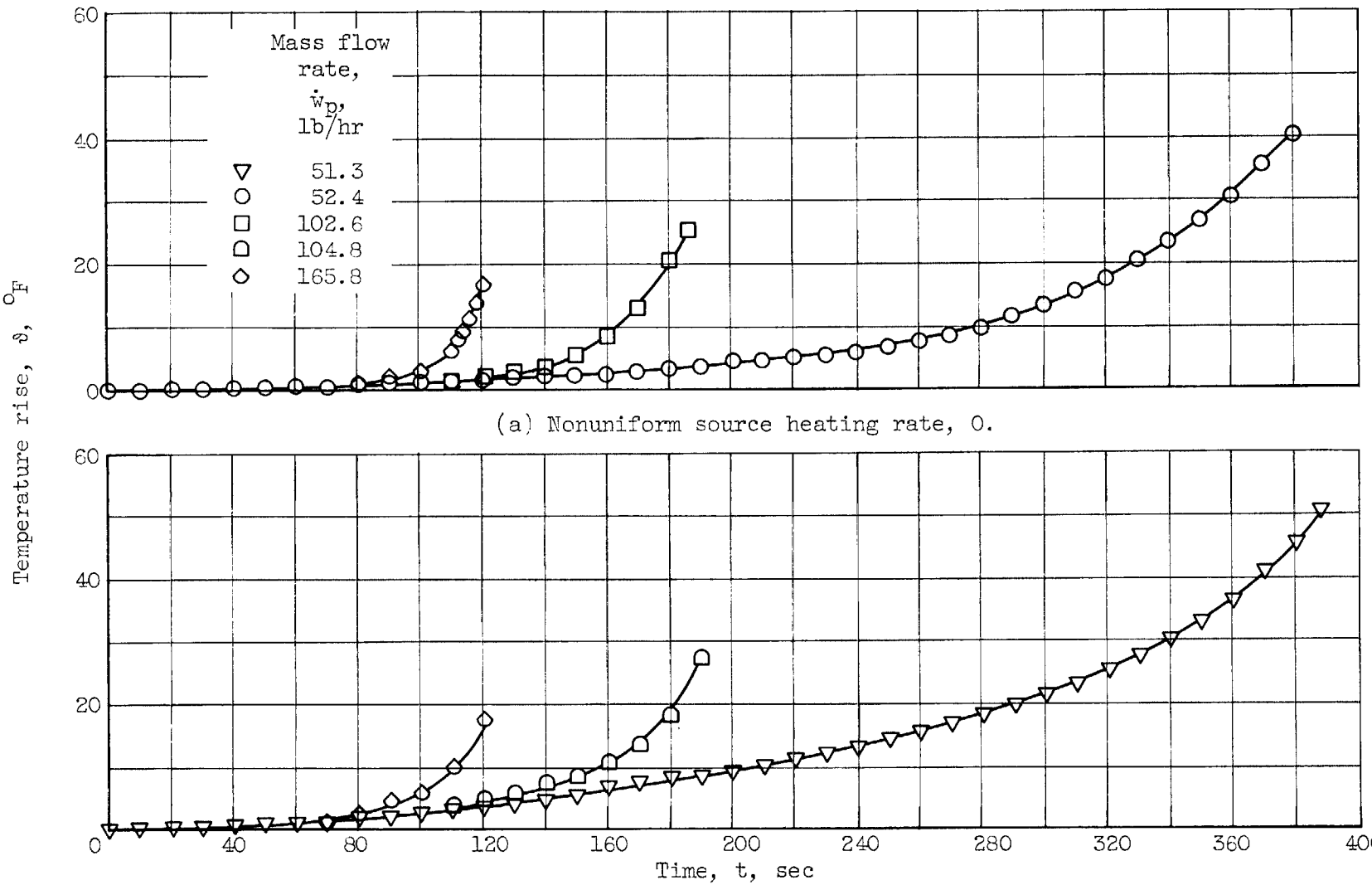

(a) Nonuniform source heating rate, 0.

(b) Nonuniform source heating rate, 163.2 Btu per hour.

Figure 18. - Temperature-time histories of outflowing fluid measured at tank exit. Wall heat flux, 15.85 Btu per square inch per hour.

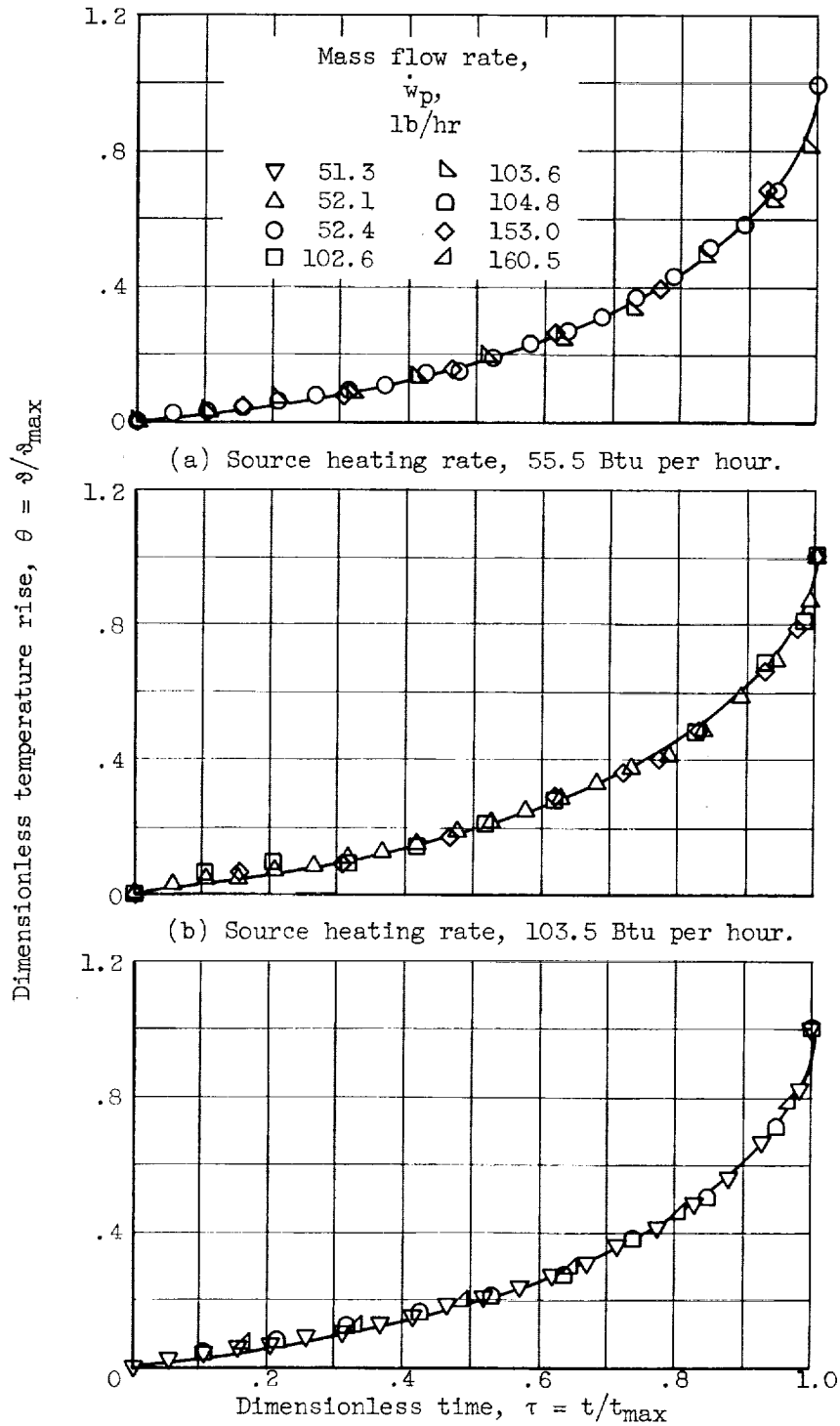

(a) Source heating rate, 55.5 Btu per hour.

(b) Source heating rate, 103.5 Btu per hour.

(c) Source heating rate, 163.2 Btu per hour.

Figure 19. - Dimensionless temperature-time histories measured at tank exit for nonuniform source heating.

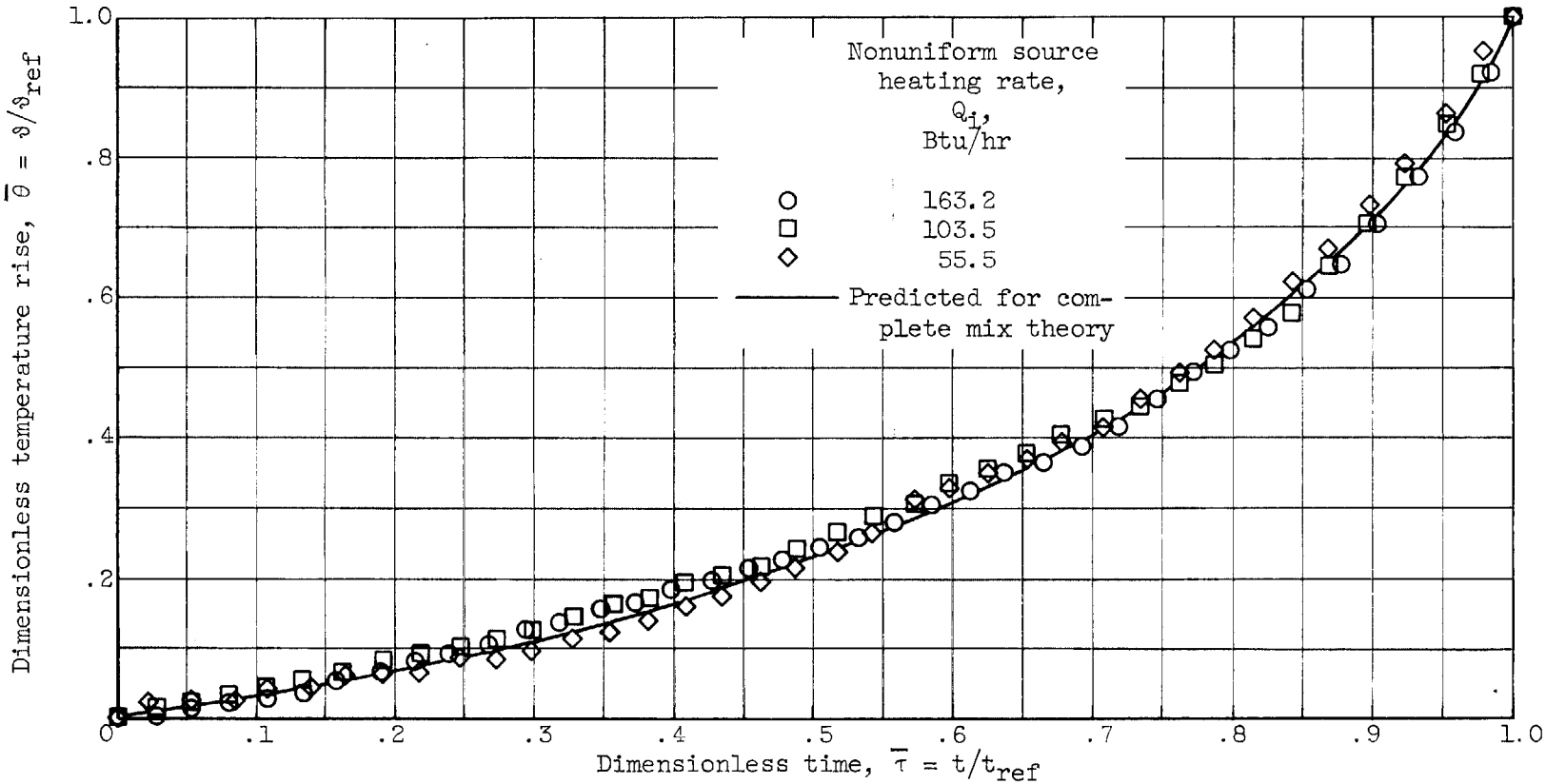

Figure 20. - Experimental and theoretical dimensionless temperature-time history of outflowing fluid at tank exit; $t_{ref} = 0.968\ t_{max}$.

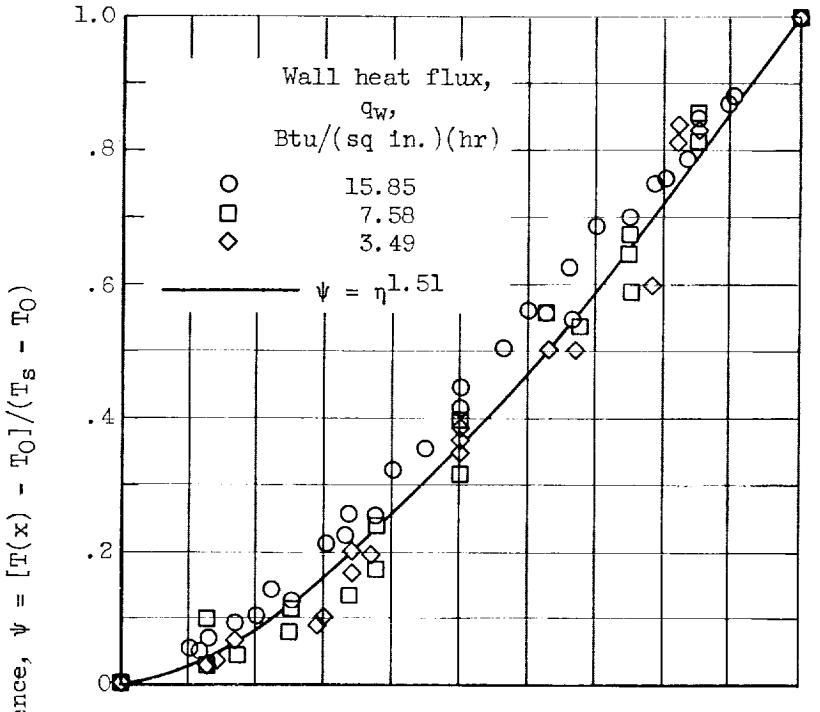

(a) Source heating rate, 0.

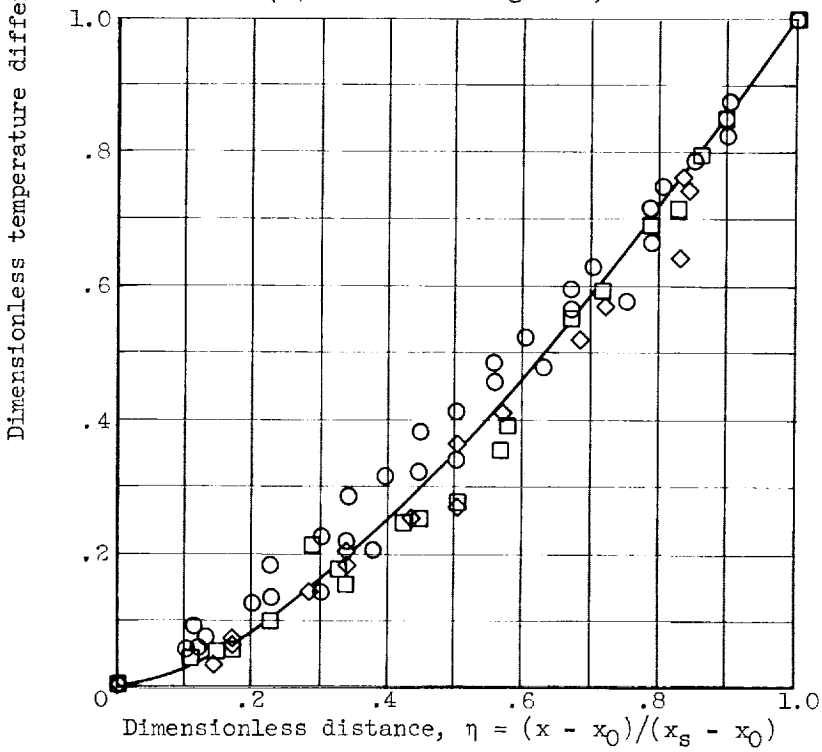

(b) Source heating rate, 163.2 Btu per hour.

Figure 21. - Dimensionless temperature profile in stratified layer.